KDM3A regulates alternative splicing of cell-cycle genes following DNA damage

Mai Baker[1], Mayra Petasny[1], Mercedes Bentata[1], Gillian Kay[1], Eden Engal[1], Yuval Nevo[1], Ahmad Siam[1], Sara Dahan[1] and Maayan Salton[1,*]

[1]Department of Biochemistry and Molecular Biology, the Institute for Medical Research Israel Canada, Faculty of Medicine, Hebrew University of Jerusalem, Jerusalem 91120, Israel

*To whom correspondence should be addressed. Tel: +972 26758814; Email: maayan.salton@mail.huji.ac.il

Running head: KDM3A regulates alternative splicing of cell-cycle genes

Keywords: pre-mRNA splicing, alternative splicing, chromatin

ABSTRACT

Changes in the cellular environment result in chromatin structure alteration, which in turn regulates gene expression. To learn about the effect of the cellular environment on the transcriptome, we studied the H3K9 de-methylase KDM3A. Using RNA-seq, we found that KDM3A regulates the transcription and alternative splicing of genes associated with cell cycle and DNA damage. We showed that KDM3A undergoes phosphorylation by PKA at serine 265 following DNA damage, and that the phosphorylation is important for a proper cell cycle regulation. We demonstrated that SAT1 alternative splicing, regulated by KDM3A, plays a role in cell cycle regulation. Furthermore we found that KDM3A's demethylase activity is not needed for SAT1 alternative splicing regulation. In addition, we identified KDM3A's protein partner ARID1A, the SWI/SNF subunit, and SRSF3 as regulators of SAT1 alternative splicing and showed that KDM3A is essential for SRSF3 binding to SAT1 pre-mRNA. These results suggest that KDM3A serves as a sensor of the environment and an adaptor for splicing factor binding. Our work reveals chromatin sensing of the environment in the regulation of alternative splicing.

INTRODUCTION

Splicing of precursor mRNA (pre-mRNA) is an important regulatory step in gene expression. The process of alternative splicing enables the production of protein isoforms from a single gene, isoforms that can have different functions, all contributing to the cell's diverse tasks[1]. Traditionally the regulation of alternative splicing was attributed to regulatory elements in the pre-mRNA. Recently we and others have shown the link between chromatin structure and epigenetic modifications in splicing regulation[2-10]. The data linking chromatin and alternative splicing is not enough to explain the physiological causes and consequences of chromatin-mediated changes in alternative splicing. Furthermore, a major unanswered question in the field is how, and to what extent, environmental changes shape the cell transcriptome via modulation of alternative splicing.

Cellular environment has been shown to modulate splicing in several ways[11,12]. The main one is the induction of post-translational modifications of splicing factors. Phosphorylation of SR splicing factors affects their protein-protein interactions as well as regulating protein activity[11]. A specific example is activation of the Fas receptor leading to dephosphorylation of SR proteins that promote pro-apoptotic isoforms of two key regulators, Bcl-X and caspase-9[13]. Another example is cell-cycle-dependent splicing patterns, which are also modulated by SR protein phosphorylation by specific kinases and phosphatases such as NIPP1[14]. Another mode of action for alternative splicing regulation following cellular environmental changes could be by modulating chromatin, as changes in the environment are sensed by cells and transduced into changes in gene expression[15], leading to specific cellular responses.

The histone demethylase KDM3A has been shown to respond to the environment to alter transcription patterns[16,17]. KDM3A's specific demethylase activity is on H3K9me1 and H3K9me2 catalyzed by histone methyltransferases EHMT2/G9a and EHMT1/GLP[18,19]. Unlike H3K9me3, which is mostly a repressive mark present in heterochromatin regions, H3K9me2 is mainly on euchromatin[18,19]. The regulation of H3K9me2 is dynamic and KDM3A is known to be regulated post-translationally in multiple ways[16,17] and thus it is suitable to be a responsive sensor for the environment.

KDM3A was shown to be phosphorylated in response to cold temperatures in adipose tissue and promote a specific expression pattern by demethylating promoters of genes important for chronic adaptation to cold stress[16]. In addition to cold shock, KDM3A is also phosphorylated on serine 265 following β-adrenergic stimulation. Interestingly, the modification promotes a scaffold function of KDM3A separate to its demethylase activity[17]. Serving as a scaffold for acetyltransferases present in enhancers and promoters allows transcription of key metabolic

62 genes[17]. Under heat shock conditions phosphorylation of KDM3A on serine 264 promotes
63 transcription of specific target genes[20]. Another response by KDM3A is to pressure-overload
64 by cardiomyocytes which promotes transcription of genes with pro-fibrotic activity[21]. In
65 addition, KDM3A responds to IL-6, androgen receptor and hypoxia[22-24].

66 KDM3A's pivotal role in transcription suggests that its misregulation could be a cause of
67 disease. Indeed upregulation of KDM3A is related to tumorigenesis of colorectal cancer cell
68 migration and invasion[25]. This function of KDM3A is attributed to its transcription of c-*Myc*,
69 cyclin D1, and *PCNA*[26,27]. In addition regulation of androgen receptor and estrogen receptor
70 transcription by KDM3A position it as a central player in prostate and breast cancer [23,28-32].

71 The role of H3K9me2 modification in alternative splicing was demonstrated by us and others.
72 While H3K9me2 modification in promoter regions have been shown to cause gene silencing,
73 the same modification in the intragenic region of genes was shown to alter alternative
74 splicing[28,33-41]. The connection of the H3K9 methylation and the spliceosome was shown to be
75 via an adaptor system containing a chromatin reader, which is one of the three HP1 proteins
76 known to bind H3K9 methylation, HP1α, β and γ[42]. The chromatin reader in turn will bind a
77 splicing factor that will recruit or block the spliceosome to promote a specific event of
78 alternative splicing[33].

79 Here we explored KDM3A's role in the cellular response to the changing environment. To this
80 end we conducted RNA-seq following silencing of KDM3A and discovered a functional
81 group of cell-cycle genes to be regulated in both expression and alternative splicing. We
82 identified protein kinase A (PKA) as the kinase that phosphorylates KDM3A serine 265
83 following DNA damage. This phosphorylation is important for KDM3A's function as a
84 scaffold joining the SWI/SNF complex and the splicing factor SRSF3 to modulate its targets.
85 We focused on one of its targets, SAT1, and showed that regulating its alternative splicing is
86 important for proper cell-cycle regulation following DNA damage. Our work exemplifies the
87 importance of alternative splicing in the cellular response to the cell's changing environment.

88

89 **RESULTS**

90 **KDM3A regulates transcription and alternative splicing of cell-cycle genes**

91 In order to learn how changes in the cellular environment result in chromatin structure
92 alteration, which in turn regulates gene expression, we silenced the prominent cellular sensor
93 histone demethylase KDM3A. Since KDM3A's role in breast cancer progression is well
94 established, we chose to use the breast cancer cell-line MCF7[31,32]. We began by characterizing

95 all KDM3A-dependent expression and alternative splicing events by means of deep RNA-
96 sequencing at a genome-wide scale using siRNA (Supplementary Fig. S1A&B). As expected
97 of a demethylase, we detected 1075 genes that are differentially expressed when KDM3A is
98 silenced (cut-off set at 1.5-fold); of these 3% were also alternatively spliced. Interestingly, we
99 found a further group of 777, which did not show changes in expression, but that were
100 alternatively spliced (Fig. 1A). This result suggests that KDM3A is a regulator of alternative
101 splicing and that alternative splicing regulation by KDM3A, directly or indirectly, is almost
102 exclusively independent of its role as a transcription regulator.

103 Among the 809 genes that were differentially spliced, we observed all types of alternative
104 splicing events: skipped exons (SE; 573 events in 477genes), alternative 5′ splice site (A5SS;
105 118 events in 109 genes), alternative 3′ splice site (A3SS; 100 events in 97 genes), mutually
106 exclusive exons (MXE; 119 events in 96 genes) and retained introns (RI; 97 events in 94 genes).
107 We chose to validate the five top-ranking candidates (SCML, HNRNPL, PTRH2, SAT1 and
108 ENSA) and found all to change in alternative splicing following silencing of KDM3A
109 (Supplementary Fig. S1C-D). Using the DAVID function annotation tool (DAVID,
110 https://david.ncifcrf.gov/)[43,44], we found that the list of differentially expressed genes was
111 enriched for genes with functions in cell cycle, cell migration and cell motility (Fig. 1B). The
112 differentially alternative spliced genes were enriched for genes involved in metabolic
113 processes, DNA repair, cell cycle, and cellular response to DNA damage (Fig. 1C). This result
114 demonstrates that while KDM3A regulates different genes in expression and alternative
115 splicing, the function of the genes in the two groups is similar. In addition these results
116 suggest a new role for KDM3A following DNA damage.

117 The DNA damage response is a cellular system that maintains genomic stability. This system
118 activates an enormous amount of proteins that efficiently modulate many physiological
119 processes. The overall cellular response to DNA damage goes far beyond repair. It modulates
120 numerous physiological processes, and alters gene expression profiles and protein synthesis,
121 degradation and trafficking. One of its hallmarks is the activation of cell-cycle checkpoints
122 that temporarily halt the cell-cycle while damage is assessed and repaired [45].

123 **KDM3A is phosphorylated by PKA following induction of double-strand breaks**

124 KDM3A phosphorylation has been shown to occur following a change in temperature[17,20].
125 Heat stress induces KDM3A S264 phosphorylation[20], whereas cold stress promotes KDM3A
126 S265 phosphorylation[17]. In order to check whether KDM3A is phosphorylated following DNA
127 damage, we began by exploring mass-spec data using phospho-site[46]. We found that KDM3A
128 S265 is phosphorylated following treatment with etoposide, a topoisomerase II inhibitor that

129 primarily causes double-strand DNA breaks[47]. To validate this mass-spec result, we induced
130 double-strand DNA breaks in MCF7 cells with the radiomimetic drug neocarzinostatin (NCS).
131 We detected KDM3A S265 phosphorylation using an antibody specific for its phospho-S265[17].
132 Our result shows that KDM3A S265 is phosphorylated while the total amount of KDM3A does
133 not change following DNA damage (Fig. 2A).

134 We continued by asking which is the kinase that phosphorylates KDM3A. While the nuclear
135 kinase ataxia telangiectasia mutated (ATM) is the main kinase activated following double-
136 strand breaks[48], the motif in KDM3A S265 does not match ATM's preference (serine followed
137 by glutamine, SQ). The motif in fact suggests that the kinase is PKA[17]. While PKA is not a
138 bona-fide DNA damage kinase, it is known to phosphorylate ataxia telangiectasia and Rad3-
139 related protein (ATR) following single-strand breaks[49]. To check whether PKA
140 phosphorylates KDM3A on S265 following double-strand breaks, we incubated MCF7 cells
141 with NCS with or without PKA inhibitor. Our results show reduced phosphorylation of
142 KDM3A S265 following inhibition of PKA, indicating that PKA indicating that PKA, or
143 another kinase phosphorylated by PKA, is KDM3A's kinase (Fig. 2B).

144 **More cells in S phase following silencing of KDM3A or mutation at its phosphorylation**
145 **site**

146 To examine KDM3A's role in cell cycle checkpoint following DNA damage, we silenced
147 KDM3A using siRNA and induced double-strand breaks with NCS. We found a mild increase
148 in percentage of cells in S-phase in cells silenced for KDM3A relative to control (Fig. S2A-C).
149 The slight change might result from redundancy of KDM3A function with other demethylases
150 such as KDM4C[50].

151 To check if phosphorylation of KDM3A S265 is important for S-phase checkpoint, we stably
152 expressed KDM3A with S265 mutated to alanine (S265A) or aspartic acid (S265D), mimicking
153 the non-phosphorylated or phosphorylated form, respectively (Supplementary Fig. S2D).
154 Comparing the cell cycle recovery in these cells to cells stably expressing WT KDM3A, we
155 found a higher percentage of cells in S-phase in S265A but not in S265D, suggesting that
156 KDM3A phosphorylation plays a role in cell cycle regulation (Fig. 2C and Supplementary Fig.
157 S2E). In addition, we monitored the cell cycle of MCF7 cells whose PKA was inhibited and
158 found a similar effect with a higher percentage of cells in S-phase (Fig. 2D and Supplementary
159 Fig. S2F). This supported the idea that PKA and KDM3A are in the same pathway in the
160 cellular response to DNA damage.

161 **SAT1, a KDM3A target in alternative splicing regulation**

162 To study KDM3A's role in cell cycle via alternative splicing, we chose to examine its target
163 gene SAT1 (Supplementary Fig. S1C). SAT1 belongs to the acetyltransferase family and is a
164 rate-limiting enzyme in the catabolic pathway of polyamine metabolism. The acetylation of
165 spermidine and spermine by SAT1 regulates the cellular levels of free spermidine/spermine
166 and is critical since a decrease in their concentrations inhibits cell proliferation while an excess
167 appears to be toxic[51]. Thus the exact amount of SAT1 is important and regulated by
168 transcription, mRNA splicing, translation, and protein stability[19]. SAT1 has seven exons, and
169 recently it was reported that exon X (present between SAT1 exon 3 and 4) undergoes
170 alternative splicing (Fig. 3A)[19]. Exon X codes for three stop codons and as a result the mRNA
171 harboring exon X is a target of the nonsense-mediated mRNA decay process[19]. This is an
172 example of an alternative splicing event that leads to a decrease in the total protein amount.
173 Our RNA-seq followed by validation demonstrated that silencing of KDM3A promoted SAT1
174 exon X inclusion (Supplementary Fig. S1C and S3A-D), which decreased the amount of stable
175 SAT1 mRNA[19]. Complementarily, overexpression of KDM3A in MCF7 cells promoted SAT1
176 exon X exclusion (Supplementary Fig. S3E&F), and in the same way, following NCS we
177 observed a slight exclusion of SAT1 exon X that was abolished by inhibition of PKA
178 (Supplementary Fig. S3G&H). This result suggests that KDM3A phosphorylation is important
179 for SAT1 alternative splicing. To provide support for this, we monitored SAT1 exon X
180 inclusion in our cells that stably expressed either S265A or S265D. We found that
181 overexpression of KDM3A in its constitutively phosphorylated form promoted SAT1 exon X
182 exclusion, similar to the alternative splicing seen following DNA damage (Supplementary
183 Fig. I&J). Next we investigated the importance of SAT1 alternative splicing to cell cycle in
184 MCF7. We silenced SAT1, mimicking inclusion of exon X. We found a higher percentage of
185 cells in S-phase resembling the effect of silencing KDM3A (Fig. 3B and Supplementary Fig.
186 S3K&L). This result suggests that KDM3A and SAT1 are working in the same pathway in the
187 cellular response to DNA damage.

188 **KDM3A serves as a scaffold to regulate SAT1 alternative splicing**

189 To understand how KDM3A regulates SAT1 alternative splicing, we first asked whether the
190 demethylase activity of KDM3A is critical for its regulation of alternative splicing. To this end,
191 we stably expressed KDM3A with a mutated demethylase domain and silenced endogenous
192 KDM3A in MCF7 cells. We found that overexpression of either WT or the demethylase mutant
193 KDM3A reduced SAT1 exon X inclusion (Fig. 3C and Supplementary Fig. S3M&N). This result
194 indicates that KDM3A's demethylase activity is not essential for alternative splicing
195 regulation and suggests that KDM3A serves as a scaffold to regulate SAT1 alternative

196 splicing. We then silenced the H3K9 methyltransferases G9a and GLP and the H3K9
197 methylations readers: HP1α, HP1β and HP1γ and monitored SAT1 alternative splicing. We
198 observed SAT1 exon X inclusion when G9a or GLP were silenced (Fig. 3D and Supplementary
199 Fig. 3O), similar to the results seen when silencing KDM3A. No change in SAT1 alternative
200 splicing was observed following silencing of H3K9 methylation readers (Supplementary Fig.
201 P&Q). This result suggests that the methylation state of H3K9 might recruit KDM3A, but that
202 KDM3A does not serve as an eraser of the modification but rather as a scaffold for splicing
203 factor binding.

204 **SRSF3 and hnRNPF promote exclusion of SAT1 exon X**

205 We hypothesize that KDM3A serves as a scaffold to recruit a splicing factor to exclude SAT1
206 exon X. Such splicing factors could be those known to act as an adaptor system connecting
207 DNA and histone methylation to the spliceosome SRSF1, SRSF3, SRSF6 and SF3B1[42] and
208 hnRNPF, which was shown to bind KDM3A and regulate alternative splicing of AR variant 7
209 (AR-V7)[28]. We silenced each of these splicing factors and found that both SRSF3 and hnRNPF
210 promote exclusion of SAT1 exon X similar to KDM3A (Fig. 4A and Supplementary Fig. S4A-
211 C). This suggests that SRSF3 and hnRNPF might be working in the same pathway as KDM3A
212 in the regulation of SAT1 alternative splicing.

213 **The SWI/SNF subunit ARID1A promotes SAT1 exon X exclusion**

214 KDM3A phosphorylation on S265 following β-adrenergic stimulation regulates gene
215 expression via the SWI/SNF complex[17]. The SWI/SNF subunit Brm was previously shown to
216 promote exon inclusion of several genes[52]. This led us to ask whether the SWI/SNF complex
217 has a role in SAT1 alternative splicing. To check our hypothesis, we asked whether ARID1A,
218 a SWI/SNF subunit binding to phospho-KDM3A[17], has a role in SAT1 alternative splicing. To
219 this end, we silenced ARID1A and found that it promoted SAT1 exon X exclusion (Fig. 4B and
220 Supplementary Fig. S4D-F). Since ARID1A, KDM3A, and SRSF3 promote SAT1 exon X
221 exclusion, it is possible that they cooperate in the alternative splicing of SAT1 exon X,
222 presumably by forming an adaptor system connecting chromatin to the spliceosome.

223 **KDM3A is important for SRSF3 binding to SAT1 pre-mRNA**

224 To check if KDM3A is needed for SRSF3 binding to SAT1 pre-mRNA, we performed RNA-
225 IP for SRSF3 following silencing of KDM3A in MCF7 cells (Supplementary Fig. S4G&H).
226 Monitoring SAT1 pre-mRNA relative to input, we found silencing of KDM3A led to a
227 reduction of approximately 75% in SRSF3 binding to SAT1 pre-mRNA (Fig. 4C). This result

228 supports the hypothesis that the two proteins functionally interact in the regulation of SAT1's
229 alternative splicing.
230

231 **MATERIALS AND METHODS**

232 **Cell culture**

233 MCF7 (ATCC Number: HTB-22) and HEK293T (ATCC Number: CRL-3216) cells were grown
234 in Dulbecco's modified Eagle's medium (DMEM) supplemented with 10% fetal bovine serum;
235 cell-lines were maintained at 37°C and 5% CO_2 atmosphere.

236 **RNA interference**

237 A pool of four siRNA oligomers per gene against KDM3A, SRSF1, SRSF3, SRSF6, HP1α, HP1β,
238 HP1γ and SF3B1 were purchased from Dharmacon; SAT1, HNRNPF and ARID1A esiRNA
239 were purchased from Sigma. MCF7 cells were grown to 20–30% confluence and transfected
240 with siRNA using TransIT-X2 transfection reagent following the manufacturer's instructions.
241 After 24 h of incubation, cell culture media was refreshed and then incubated for an additional
242 48-72 h. Knockdown efficiencies were verified by qPCR.

243 **qRT-PCR**

244 RNA was isolated from cells using the GENEzol TriRNA Pure Kit (GeneAid). cDNA synthesis
245 was carried out with the Quanta cDNA Reverse Transcription Kit (QuantaBio). Then, qPCR
246 was performed with the iTaq Supermix (BioRad) on the Biorad iCycler. The comparative Ct
247 method was employed to quantify transcripts, and delta Ct was measured in triplicate.
248 Primers used to amplify the target genes are provided in Supplementary Table 1.

249 **RNA-seq**

250 RNA ScreenTape kit (catalog #5067-5576; Agilent Technologies), D1000 ScreenTape kit
251 (catalog #5067-5582; Agilent Technologies), Qubit RNA HS Assay kit (catalog # Q32852;
252 Invitrogen), and Qubit DNA HS Assay kit (catalog #32854; Invitrogen) were used for each
253 specific step for quality control and quantity determination of RNA and library preparation.
254 For mRNA library preparation: TruSeq RNA Library Prep Kit v2 was used (Illumina). In brief,
255 1 μg was used for the library construction; library was eluted in 20 μL of elution buffer.
256 Libraries were adjusted to 10 mM, and then 10 μL (50%) from each sample was collected and
257 pooled in one tube. Multiplex sample pool (1.5 pM including PhiX 1.5%) was loaded in
258 NextSeq 500/550 High Output v2 kit (75 cycles cartridge and 150 cycles cartridge; Illumina).
259 Run conditions were in paired end (43 × 43 bp and 80 × 80 bp, respectively) and loaded on

260 NextSeq 500 System machine (Illumina). We used rMATS (version3.2.5)[53] to identify
261 differential alternative splicing events between the two sample groups corresponding to all
262 five basic types of alternative splicing patterns. Briefly, rMATS uses a modified version of the
263 generalized linear mixed model to detect differential alternative splicing from RNA-seq data
264 with replicates, while controlling for changes in overall gene expression levels. It accounts for
265 exon-specific sequencing coverage in individual samples as well as variation in exon splicing
266 levels among replicates. For each alternative splicing event, we used the calculation on both
267 the reads mapped to the splice junctions and the reads mapped to the exon body. The results
268 of rMATS analysis gave low numbers of significant AS events with p-value 0.05 and a cut off
269 at FDR < 5%. Thus, one replicate was excluded from the analysis, and then specific parameters
270 were identified manually; with inclusion level difference between groups = 2, and average
271 count >10.

272 **Viral infection**

273 Retroviral or lentiviral particles were produced by expressing KDM3A-P S265 WT or mutants
274 (S265A, S265D)[17] or p-Lenti-V5-KDM3A-WT (addgene #82331) or demethylase MUT
275 (addgene #82332) plasmids respectively in the HEK293T packaging cell-line using TransIT-
276 X2 transfection reagent. MCF7 cells were infected with viral particles and stable integrations
277 were selected.

278 **Immunoblotting and immunoprecipitation**

279 For immunoblotting cells were harvested and lysed with RIPA lysis buffer, and the extracts
280 were run on a 4–12% Bis-Tris gel and transferred onto a polyvinylidene difluoride membrane.
281 For immunoprecipitation cells were washed twice with ice-cold PBS, harvested and lysed for
282 30 min on ice in 0.5% NP40, 150 mM NaCl, 50 Mm Tris pH7.5, and 2 mM MgCl2 supplemented
283 with protease, phosphatase and RNase inhibitors. Supernatants were collected after
284 centrifugation at 21, 000 g for 20 min. Supernatants were immunoprecipitated for 2 h with 40
285 ul of anti-Flag M2 Magnetic Beads (M8823, Sigma Aldrich). Beads were washed sequentially
286 for 5 min. Beads were boiled in sample buffer and loaded onto the gel for analysis. The
287 samples were subjected to standard immunoblotting analysis using polyvinylidene difluoride
288 membranes and enhanced chemiluminescence.

289 **Antibodies**

290 Antibodies used for immunoblotting were KDM3A-Ser265 (Kindly supplied by Dr. Juro
291 Sakai, RCAST, University of Tokyo), KDM3A (cat# ab106456, Abcam), Arid1A (cat# sc-32761,

292 Santa Cruz Biotechnology), SRSF3 (cat# sc-13510, Santa Cruz Biotechnology), SAT1 (D1T7M,
293 cat# 61586, Cell Signaling Technology).

294 **Flow cytometry**

295 Cells were trypsinized, washed with PBS, fixed overnight at -20°C with 70% ethanol in PBS,
296 washed with PBS, and left for 30 min at 4°C. The cell suspension was then incubated with PBS
297 containing 5 μg/ml DNase-free RNase and stained with propidium iodide (PI). Data was
298 acquired using LSRII Fortessa analyser machine at 10,000 events/sample. The percentage of
299 cells in each cell cycle phase was determined using Flow Jo software.

300 **Chemical reagents**

301 Neocarzinostatin (NCS) was obtained from Sigma (Ca# 067M4060V). PKA inhibitor was
302 obtained from Sigma (P6062).

303 **RNA-immunoprecipitation (RNA-IP)**

304 Cells were washed with ice-cold PBS, harvested, and lysed for 30 min on ice in a buffer
305 containing 1% NP40 150 mM NaCl, 50 mM Tris pH = 7.5, and 1 mM EDTA supplemented
306 with protease and RNAsin inhibitors followed by sonication in an ultrasonic bath (Qsonica,
307 Q800R2 Sonicator) for 6 cycles of 5 s ON and 30 s OFF. Supernatants were collected after
308 centrifugation at 21,000 g for 20 min. Antibody was added for 2 h at 4°C. Protein A and G
309 sepharose beads were added for an additional 1 h. Beads were washed 4 times and GeneZol
310 added for RNA extraction. Serial dilutions of the 10% input cDNA (1:5, 1:25, 1:125) were
311 analyzed by SYBR-Green real-time qPCR. The oligonucleotide sequences used are listed in
312 Supplementary Table S1.

313

314 **DISCUSSION**

315 Chromatin structure is constantly changing in response to the cell's environment. These
316 dynamic alterations are the basis of a changing cellular transcriptome that in turn adjust the
317 cell to the new environment. Here we suggest a transcriptome change by alternative splicing
318 giving rise to isoforms that are better able to respond to the environment. To this end we
319 studied the role of the signal-sensing scaffold KDM3A. While KDM3A's role in temperature
320 sensing is well established, we have now found that it is phosphorylated following DNA
321 damage to regulate alternative splicing, as well as the expression of cell cycle genes.

322 DNA damage has been shown multiple times by us and others to regulate the transcriptome
323 and specifically alternative splicing[54-57]. Here we add that the mediator of the alternative

splicing regulation can be chromatin proteins that are a known part of the massive cellular response to DNA damage. Splicing factors were also demonstrated to be part of the signal transduction following DNA damage. In particular SRSF3 was demonstrated to serve as a regulator of genome integrity and cell cycle[58-61]. Our work demonstrates that chromatin alternations following DNA damage could serve as a scaffold to recruit SRSF3 to specific cell cycle genes. This observation could add a level of regulation to splicing factors' preference for their targets following a cellular environment change.

Histone modifications over alternatively spliced gene regions have previously been shown to act as recognition sites for epigenetic adaptor proteins, which in turn recruit splicing factors[4,33]. Here we demonstrate that phosphorylated S265 KDM3A itself could serves as a scaffold for splicing factor recruitment with the SWI/SNF subunit ARID1A. Another subunit of the SWI/SNF complex, Brm, was indicated to regulate alternative splicing by promoting inclusion of exons via slowing down of RNA polymerase II elongation[52]. However, our results show that ARID1A promotes exclusion of SAT1 exon X. This suggest that the mechanism of the SWI/SNF complex on the SAT1 gene is different to that described before.

Our results demonstrate that the H3K9me2 methyltransferases, G9a and GLP, and its demethylase, KDM3A, both promote exclusion of SAT1 exon X. This result is of special interest and provide strong evidence that KDM3A serves as the scaffold, and not the H3K9 modification, for recruiting SRSF3. Our previous work found HP1γ to bind H3K9me2 and recruit the splicing factor SRSF1[33]. This model suggests that KDM3A enzymatic activity will abolish this adaptor system and will promote the opposite alternative splicing outcome. However, SAT1 is a proof that G9a and KDM3A can work in a similar way to regulate alternative splicing. A deeper investigation is needed to learn the fine tuning of each of these chromatin factors.

Demethylation of H3K9 by KDM3A was shown to promote alternative splicing of AR7 by recruiting hnRNPF[28]. This work describes a mechanism that is distinct from the one we describe here as it requires KDM3A's enzymatic activity and our work shows that the methylase mutant of KDM3A can also serve as an alternative splicing regulator. Our results shed light on the many mechanisms by which chromatin can regulate alternative splicing.

DATA AVAILABILITY

The RNA-seq data has been deposited to the Gene Expression Omnibus (GEO) with the dataset identifier GSE141948.

ACKNOWLEDGEMENTS

We thank Prof. Juro Sakai and Prof. Takeshi Inagaki for plasmids and p-KDM3A antibody. We thank Abed Nasereddin and Idit Shiff from the Genomic Applications Laboratory, The Core Research Facility, The Faculty of Medicine - Ein Kerem, The Hebrew University of Jerusalem, Israel, for their professional advice and RNA-seq service.

This work was in part supported by the Alon Award by the Israeli Planning and Budgeting Committee (PBC) and the Israel Science Foundation (ISF 1154/17). The RNA-seq reagents were funded by a Core Lab Grant Program launched by Danyel Biotech, the authorized Illumina Channel Partner in Israel.

CONFLICTS OF INTEREST

The authors declare no conflicts of interest

REFERENCES

1 Keren, H., Lev-Maor, G. & Ast, G. Alternative splicing and evolution: diversification, exon definition and function. *Nat Rev Genet* **11**, 345-355, doi:10.1038/nrg2776 (2010).

2 Schwartz, S., Meshorer, E. & Ast, G. Chromatin organization marks exon-intron structure. *Nature structural & molecular biology* **16**, 990-995, doi:10.1038/nsmb.1659 (2009).

3 Luco, R. F. *et al.* Regulation of alternative splicing by histone modifications. *Science* **327**, 996-1000, doi:10.1126/science.1184208 (2010).

4 Luco, R. F., Allo, M., Schor, I. E., Kornblihtt, A. R. & Misteli, T. Epigenetics in alternative pre-mRNA splicing. *Cell* **144**, 16-26, doi:10.1016/j.cell.2010.11.056 (2011).

5 Tilgner, H. *et al.* Nucleosome positioning as a determinant of exon recognition. *Nature structural & molecular biology* **16**, 996-1001, doi:10.1038/nsmb.1658 (2009).

6 Kolasinska-Zwierz, P. *et al.* Differential chromatin marking of introns and expressed exons by H3K36me3. *Nat Genet* **41**, 376-381, doi:10.1038/ng.322 (2009).

7 Hnilicova, J. & Stanek, D. Where splicing joins chromatin. *Nucleus* **2**, 182-188, doi:10.4161/nucl.2.3.15876 (2011).

8 Haque, N. & Oberdoerffer, S. Chromatin and splicing. *Methods Mol Biol* **1126**, 97-113, doi:10.1007/978-1-62703-980-2_7 (2014).

9 Kornblihtt, A. R., Schor, I. E., Allo, M. & Blencowe, B. J. When chromatin meets splicing. *Nature structural & molecular biology* **16**, 902-903 (2009).

10 Siam, A. *et al.* Regulation of alternative splicing by p300-mediated acetylation of splicing factors. *RNA* **25**, 813-824, doi:10.1261/rna.069856.118 (2019).

11 Ghosh, G. & Adams, J. A. Phosphorylation mechanism and structure of serine-arginine protein kinases. *FEBS J* **278**, 587-597, doi:10.1111/j.1742-4658.2010.07992.x (2011).

12 Pozzi, B., Mammi, P., Bragado, L., Giono, L. E. & Srebrow, A. When SUMO met splicing. *RNA Biol* **15**, 689-695, doi:10.1080/15476286.2018.1457936 (2018).
13 Chalfant, C. E. *et al.* De novo ceramide regulates the alternative splicing of caspase 9 and Bcl-x in A549 lung adenocarcinoma cells. Dependence on protein phosphatase-1. *The Journal of biological chemistry* **277**, 12587-12595, doi:10.1074/jbc.M112010200 (2002).
14 Trinkle-Mulcahy, L. *et al.* Nuclear organisation of NIPP1, a regulatory subunit of protein phosphatase 1 that associates with pre-mRNA splicing factors. *J Cell Sci* **112 (Pt 2)**, 157-168 (1999).
15 Fang, L. *et al.* Environmental-stress-induced Chromatin Regulation and its Heritability. *J Carcinog Mutagen* **5**, doi:10.4172/2157-2518.1000156 (2014).
16 Abe, Y. *et al.* Histone demethylase JMJD1A coordinates acute and chronic adaptation to cold stress via thermogenic phospho-switch. *Nat Commun* **9**, 1566, doi:10.1038/s41467-018-03868-8 (2018).
17 Abe, Y. *et al.* JMJD1A is a signal-sensing scaffold that regulates acute chromatin dynamics via SWI/SNF association for thermogenesis. *Nat Commun* **6**, 7052, doi:10.1038/ncomms8052 (2015).
18 Yamane, K. *et al.* JHDM2A, a JmjC-containing H3K9 demethylase, facilitates transcription activation by androgen receptor. *Cell* **125**, 483-495, doi:10.1016/j.cell.2006.03.027 (2006).
19 Hyvonen, M. T. *et al.* Polyamine-regulated unproductive splicing and translation of spermidine/spermine N1-acetyltransferase. *Rna* **12**, 1569-1582, doi:10.1261/rna.39806 (2006).
20 Cheng, M. B. *et al.* Specific phosphorylation of histone demethylase KDM3A determines target gene expression in response to heat shock. *PLoS Biol* **12**, e1002026, doi:10.1371/journal.pbio.1002026 (2014).
21 Zhang, Q. J. *et al.* Histone lysine dimethyl-demethylase KDM3A controls pathological cardiac hypertrophy and fibrosis. *Nat Commun* **9**, 5230, doi:10.1038/s41467-018-07173-2 (2018).
22 Kim, H. *et al.* KDM3A histone demethylase functions as an essential factor for activation of JAK2-STAT3 signaling pathway. *Proceedings of the National Academy of Sciences of the United States of America* **115**, 11766-11771, doi:10.1073/pnas.1805662115 (2018).
23 Wilson, S., Fan, L., Sahgal, N., Qi, J. & Filipp, F. V. The histone demethylase KDM3A regulates the transcriptional program of the androgen receptor in prostate cancer cells. *Oncotarget* **8**, 30328-30343, doi:10.18632/oncotarget.15681 (2017).
24 Krieg, A. J. *et al.* Regulation of the histone demethylase JMJD1A by hypoxia-inducible factor 1 alpha enhances hypoxic gene expression and tumor growth. *Mol Cell Biol* **30**, 344-353, doi:10.1128/MCB.00444-09 (2010).
25 Liu, J., Liang, T. & Zhangsun, W. KDM3A is associated with tumor metastasis and modulates colorectal cancer cell migration and invasion. *Int J Biol Macromol* **126**, 318-325, doi:10.1016/j.ijbiomac.2018.12.105 (2019).
26 Li, X. *et al.* A potential common role of the Jumonji C domain-containing 1A histone demethylase and chromatin remodeler ATRX in promoting colon cancer. *Oncol Lett* **16**, 6652-6662, doi:10.3892/ol.2018.9487 (2018).
27 Peng, K. *et al.* Histone demethylase JMJD1A promotes colorectal cancer growth and metastasis by enhancing Wnt/beta-catenin signaling. *The Journal of biological chemistry* **293**, 10606-10619, doi:10.1074/jbc.RA118.001730 (2018).

28 Fan, L. *et al.* Histone demethylase JMJD1A promotes alternative splicing of AR variant 7 (AR-V7) in prostate cancer cells. *Proc Natl Acad Sci U S A* **115**, E4584-E4593, doi:10.1073/pnas.1802415115 (2018).
29 Fan, L. *et al.* Regulation of c-Myc expression by the histone demethylase JMJD1A is essential for prostate cancer cell growth and survival. *Oncogene* **35**, 2441-2452, doi:10.1038/onc.2015.309 (2016).
30 Yao, J., Zheng, S., Li, B., Li, X. & Liu, W. KDM3A is not associated with metastasis and prognosis of breast cancer. *Oncol Lett* **15**, 9751-9756, doi:10.3892/ol.2018.8578 (2018).
31 Ramadoss, S., Guo, G. & Wang, C. Y. Lysine demethylase KDM3A regulates breast cancer cell invasion and apoptosis by targeting histone and the non-histone protein p53. *Oncogene* **36**, 47-59, doi:10.1038/onc.2016.174 (2017).
32 Wade, M. A. *et al.* The histone demethylase enzyme KDM3A is a key estrogen receptor regulator in breast cancer. *Nucleic Acids Res* **43**, 196-207, doi:10.1093/nar/gku1298 (2015).
33 Salton, M., Voss, T. C. & Misteli, T. Identification by high-throughput imaging of the histone methyltransferase EHMT2 as an epigenetic regulator of VEGFA alternative splicing. *Nucleic Acids Res* **42**, 13662-13673, doi:10.1093/nar/gku1226 (2014).
34 Fiszbein, A. & Kornblihtt, A. R. Histone methylation, alternative splicing and neuronal differentiation. *Neurogenesis (Austin)* **3**, e1204844, doi:10.1080/23262133.2016.1204844 (2016).
35 Fiszbein, A. *et al.* Alternative Splicing of G9a Regulates Neuronal Differentiation. *Cell Rep* **14**, 2797-2808, doi:10.1016/j.celrep.2016.02.063 (2016).
36 Agirre, E. *et al.* A chromatin code for alternative splicing involving a putative association between CTCF and HP1alpha proteins. *BMC Biol* **13**, 31, doi:10.1186/s12915-015-0141-5 (2015).
37 Schor, I. E., Fiszbein, A., Petrillo, E. & Kornblihtt, A. R. Intragenic epigenetic changes modulate NCAM alternative splicing in neuronal differentiation. *EMBO J* **32**, 2264-2274, doi:10.1038/emboj.2013.167 (2013).
38 Bieberstein, N. I. *et al.* TALE-directed local modulation of H3K9 methylation shapes exon recognition. *Sci Rep* **6**, 29961, doi:10.1038/srep29961 (2016).
39 Leisegang, M. S. *et al.* The histone demethylase PHF8 facilitates alternative splicing of the histocompatibility antigen HLA-G. *FEBS Lett* **593**, 487-498, doi:10.1002/1873-3468.13337 (2019).
40 Lev Maor, G., Yearim, A. & Ast, G. The alternative role of DNA methylation in splicing regulation. *Trends Genet* **31**, 274-280, doi:10.1016/j.tig.2015.03.002 (2015).
41 Shayevitch, R., Askayo, D., Keydar, I. & Ast, G. The importance of DNA methylation of exons on alternative splicing. *RNA* **24**, 1351-1362, doi:10.1261/rna.064865.117 (2018).
42 Yearim, A. *et al.* HP1 is involved in regulating the global impact of DNA methylation on alternative splicing. *Cell Rep* **10**, 1122-1134, doi:10.1016/j.celrep.2015.01.038 (2015).
43 Huang da, W., Sherman, B. T. & Lempicki, R. A. Systematic and integrative analysis of large gene lists using DAVID bioinformatics resources. *Nat Protoc* **4**, 44-57, doi:10.1038/nprot.2008.211 (2009).
44 Huang da, W., Sherman, B. T. & Lempicki, R. A. Bioinformatics enrichment tools: paths toward the comprehensive functional analysis of large gene lists. *Nucleic acids research* **37**, 1-13, doi:10.1093/nar/gkn923 (2009).
45 Lanz, M. C., Dibitetto, D. & Smolka, M. B. DNA damage kinase signaling: checkpoint and repair at 30 years. *EMBO J*, e101801, doi:10.15252/embj.2019101801 (2019).

494 46 Hornbeck, P. V. *et al.* PhosphoSitePlus, 2014: mutations, PTMs and recalibrations.
495 *Nucleic Acids Res* **43**, D512-520, doi:10.1093/nar/gku1267 (2015).
496 47 Beli, P. *et al.* Proteomic investigations reveal a role for RNA processing factor
497 THRAP3 in the DNA damage response. *Mol Cell* **46**, 212-225,
498 doi:10.1016/j.molcel.2012.01.026 (2012).
499 48 Shiloh, Y. & Ziv, Y. The ATM protein kinase: regulating the cellular response to
500 genotoxic stress, and more. *Nat Rev Mol Cell Biol* **14**, 197-210, doi:10.1038/nrm3546
501 (2013).
502 49 Jarrett, S. G. *et al.* PKA-mediated phosphorylation of ATR promotes recruitment of
503 XPA to UV-induced DNA damage. *Mol Cell* **54**, 999-1011,
504 doi:10.1016/j.molcel.2014.05.030 (2014).
505 50 Huang, B. *et al.* KDM3A and KDM4C Regulate Mesenchymal Stromal Cell
506 Senescence and Bone Aging via Condensin-mediated Heterochromatin
507 Reorganization. *iScience* **21**, 375-390, doi:10.1016/j.isci.2019.10.041 (2019).
508 51 Bae, D. H., Lane, D. J. R., Jansson, P. J. & Richardson, D. R. The old and new
509 biochemistry of polyamines. *Biochim Biophys Acta Gen Subj* **1862**, 2053-2068,
510 doi:10.1016/j.bbagen.2018.06.004 (2018).
511 52 Batsche, E., Yaniv, M. & Muchardt, C. The human SWI/SNF subunit Brm is a regulator
512 of alternative splicing. *Nat Struct Mol Biol* **13**, 22-29, doi:10.1038/nsmb1030 (2006).
513 53 Shen, S. *et al.* rMATS: robust and flexible detection of differential alternative splicing
514 from replicate RNA-Seq data. *Proc Natl Acad Sci U S A* **111**, E5593-5601,
515 doi:10.1073/pnas.1419161111 (2014).
516 54 Salton, M. *et al.* Matrin 3 binds and stabilizes mRNA. *PLoS One* **6**, e23882,
517 doi:10.1371/journal.pone.0023882 (2011).
518 55 Salton, M., Lerenthal, Y., Wang, S. Y., Chen, D. J. & Shiloh, Y. Involvement of Matrin
519 3 and SFPQ/NONO in the DNA damage response. *Cell Cycle* **9**, 1568-1576,
520 doi:10.4161/cc.9.8.11298 (2010).
521 56 Munoz, M. J. *et al.* DNA damage regulates alternative splicing through inhibition of
522 RNA polymerase II elongation. *Cell* **137**, 708-720, doi:10.1016/j.cell.2009.03.010
523 (2009).
524 57 Mikolaskova, B. *et al.* Maintenance of genome stability: the unifying role of
525 interconnections between the DNA damage response and RNA-processing pathways.
526 *Curr Genet* **64**, 971-983, doi:10.1007/s00294-018-0819-7 (2018).
527 58 Ajiro, M., Jia, R., Yang, Y., Zhu, J. & Zheng, Z. M. A genome landscape of SRSF3-
528 regulated splicing events and gene expression in human osteosarcoma U2OS cells.
529 *Nucleic Acids Res* **44**, 1854-1870, doi:10.1093/nar/gkv1500 (2016).
530 59 Jimenez, M. *et al.* Splicing events in the control of genome integrity: role of SLU7 and
531 truncated SRSF3 proteins. *Nucleic Acids Res* **47**, 3450-3466, doi:10.1093/nar/gkz014
532 (2019).
533 60 Kurokawa, K. *et al.* Downregulation of serine/arginine-rich splicing factor 3 induces
534 G1 cell cycle arrest and apoptosis in colon cancer cells. *Oncogene* **33**, 1407-1417,
535 doi:10.1038/onc.2013.86 (2014).
536 61 He, X. & Zhang, P. Serine/arginine-rich splicing factor 3 (SRSF3) regulates
537 homologous recombination-mediated DNA repair. *Mol Cancer* **14**, 158,
538 doi:10.1186/s12943-015-0422-1 (2015).
539

540 **Figure Legends**

541 Figure 1. **KDM3A is a regulator of transcription and alternative splicing of cell cycle and**
542 **DNA damage genes.** MCF7 cells were transfected with non-targeting siRNA (siNT) and
543 siKDM3A for 72 h. RNA was extracted, libraries prepared and RNA-seq was conducted. **A**.
544 Venn diagram representing differentially expressed genes (blue) and alternatively spliced
545 genes (red). **B & C**. Functional analysis was conducted using the DAVID functional
546 annotation tool (DAVID, https://david.ncifcrf.gov/) for (**B**) differentially expressed genes
547 and (**C**) alternative splicing genes.

548 Figure 2. **KDM3A is phosphorylated by PKA following double strand breaks. A**. MCF7 cells
549 treated with 200 ng/ml NCS for 1 h. Immunoblotting was conducted with the indicated
550 antibodies. **B**. MCF7 cells were treated with PKAi for 30 min following treatment with 50 and
551 200 ng/ml NCS for 1 h. Immunoblotting was conducted with the indicated antibodies. **C**.
552 MCF7 cells stably expressing either wild-type KDM3A or KDM3A mutated at serine 265 to
553 alanine (S265A) or to aspartic acid (S265D) were incubated with 200 ng/ml NCS, and analyzed
554 8 h later using flow cytometry. The amount of cells accumulated in S-phase is shown as a fold-
555 change relative to untreated cells. **D**. MCF7 cells were incubated with PKAi for 30 min
556 followed by treatment with 200 ng/ml NCS, and analyzed 8 h later using flow cytometry. The
557 amount of cells accumulated in S-phase is shown as a fold-change relative to untreated cells.
558 C and D, plot represents the mean of four independent experiments and ±SD (* $p<0.05$; **
559 $p<0.01$).

560 Figure 3. **KDM3A regulates SAT1 alternative splicing independent of its demethylase**
561 **enzymatic activity. A**. Schematic representation of SAT1 alternative splicing. Rectangles:
562 exons, black lines: introns. **B**. MCF7 cells were transfected with non-targeting siRNA (siNT)
563 and siSAT1 for 72 h, followed by treatment with 200 ng/ml NCS, and analyzed 8 h later using
564 flow cytometry. The amount of cells accumulated in S-phase is shown as a fold-change
565 relative to untreated cells. **C**. MCF7 cells stably expressing either the empty vector, wild-type
566 KDM3A or KDM3A mutated demethylase (mut). Total RNA was extracted and analyzed by
567 real-time PCR for SAT1 exon X inclusion. PSI was calculated by SAT1 exon X relative to SAT1
568 total mRNA amount. **D**. MCF7 cells were transfected with non-targeting siRNA (siNT) and
569 siG9a or siGLP for 72 h. Total RNA was extracted and analyzed by real-time PCR for SAT1
570 exon X inclusion. PSI was calculated by SAT1 exon X relative to SAT1 total mRNA amount.
571 Values represent averages of three independent experiments ±SD (* $p<0.05$; ** $p<0.01$; ***
572 $p<0.001$; **** $p<0.0001$).

573 Figure 4. **KDM3A allows for SRSF3 binding to SAT1 pre-mRNA. A**. MCF7 cells were
574 transfected with non-targeting siRNA (siNT) or siSF3B1, siSRSF1/3/6 and sihnRNPF for 72

575 h. Total RNA was extracted and analyzed by real-time PCR for SAT1 exon X inclusion. PSI
576 was calculated by SAT1 exon X relative to SAT1 total mRNA amount. **B**. MCF7 cells were
577 transfected with non-targeting siRNA (siNT) or siARID1A for 72 h. Total RNA was extracted
578 and analyzed by real-time PCR for SAT1 exon X inclusion. PSI was calculated by SAT1 exon
579 X relative to SAT1 total mRNA amount. **C**. MCF7 cells stably expressing FLAG-KDM3A-V5
580 were treated with 200ng/ml NCS for half an hour. KDM3A was immunoprecipitated using
581 the Flag tag, and detected with V5 (for KDM3A) and SRSF3. * long exposure. **D**. RNA-IP of
582 SRSF3 in MCF7 cells that were transfected with non-targeting siRNA (siNT) or siKDM3A for
583 72 h. Real-time PCR analysis of SAT1 intron 3 (near exon X) relative to input. Values represent
584 averages of three independent experiments ±SD (* $p<0.05$; ** $p<0.01$; **** $p<0.0001$).

585

Fig 1.

A

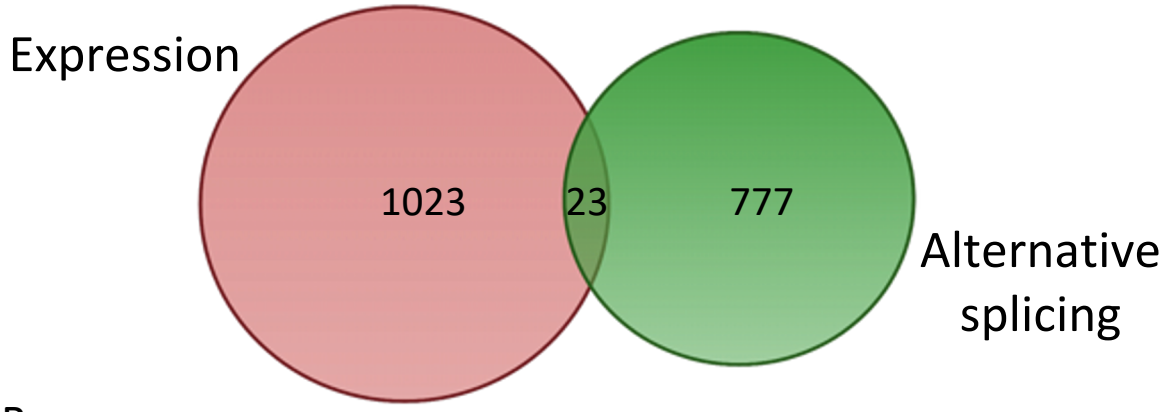
Expression
1023
23
777
Alternative splicing

B

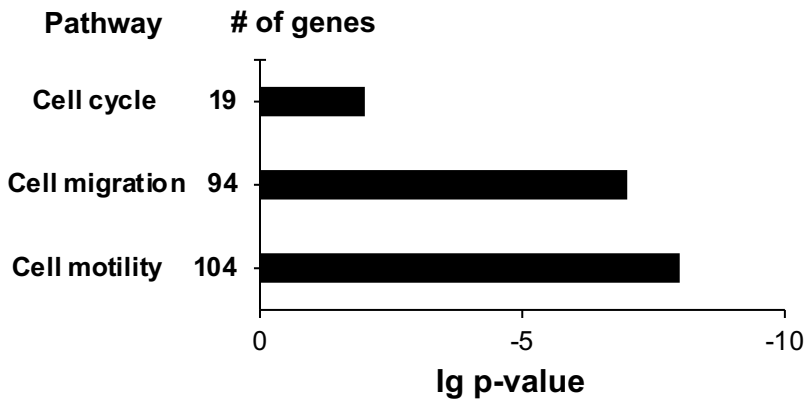
Pathway
# of genes
Cell cycle 19
Cell migration 94
Cell motility 104
0
-5
-10
lg p-value

C

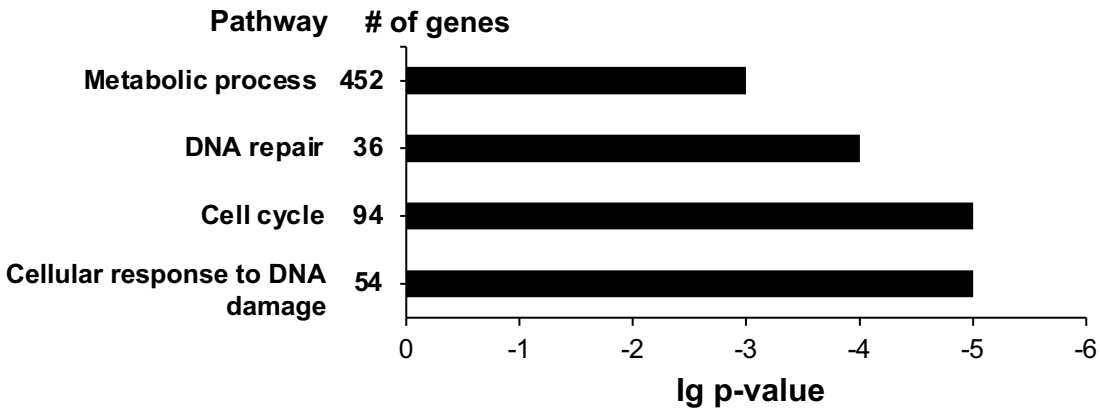
Pathway
# of genes
Metabolic process 452
DNA repair 36
Cell cycle 94
Cellular response to DNA damage 54
0
-1
-2
-3
-4
-5
-6
lg p-value

Fig 2.

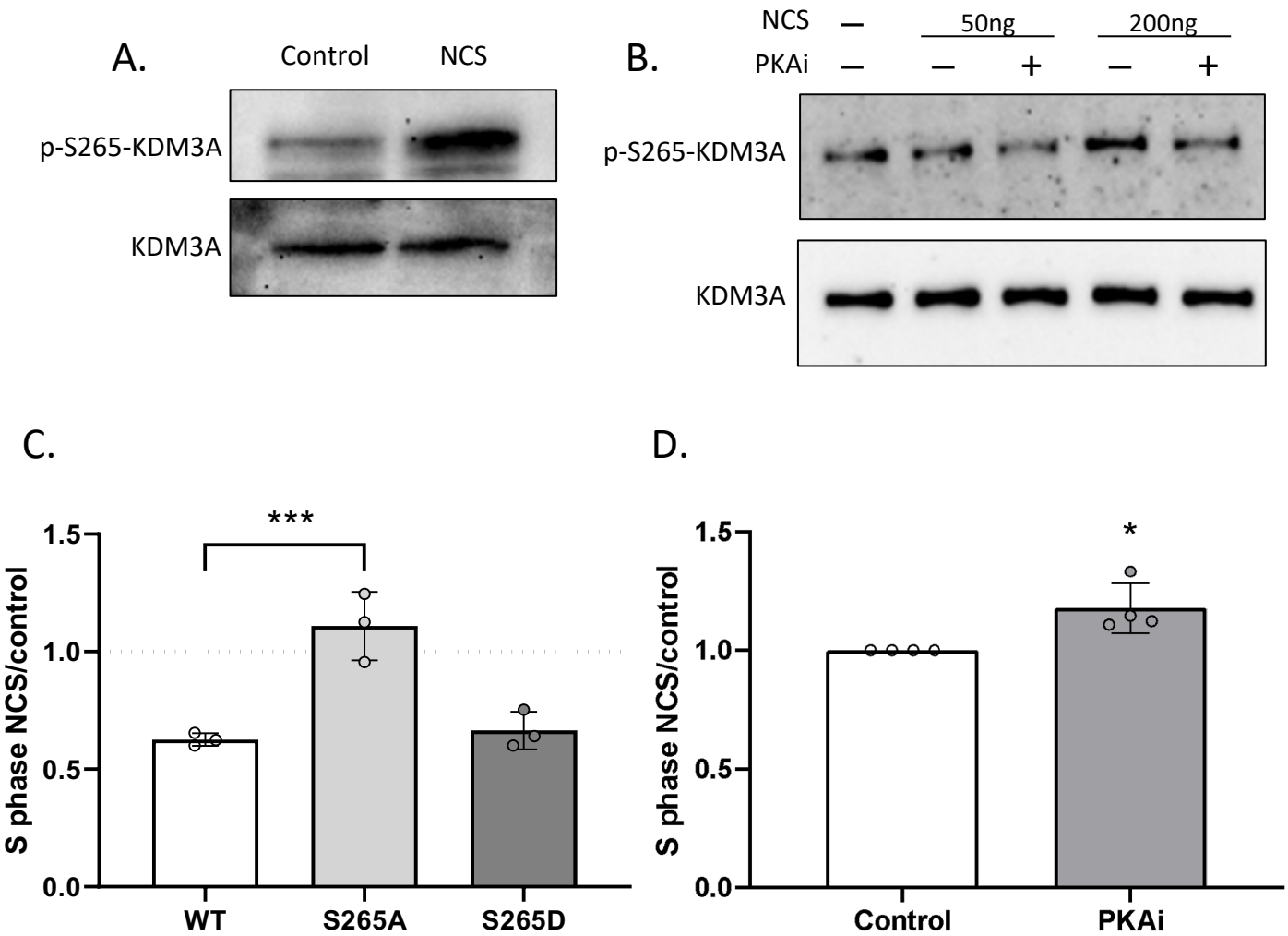
A.
Control
NCS
p-S265-KDM3A
KDM3A
B.
NCS
PKAi
50ng
200ng
p-S265-KDM3A
KDM3A
C.
***
S phase NCS/control
1.5
1.0
0.5
0.0
WT
S265A
S265D
D.
*
S phase NCS/control
1.5
1.0
0.5
0.0
Control
PKAi

Fig 3.

A.

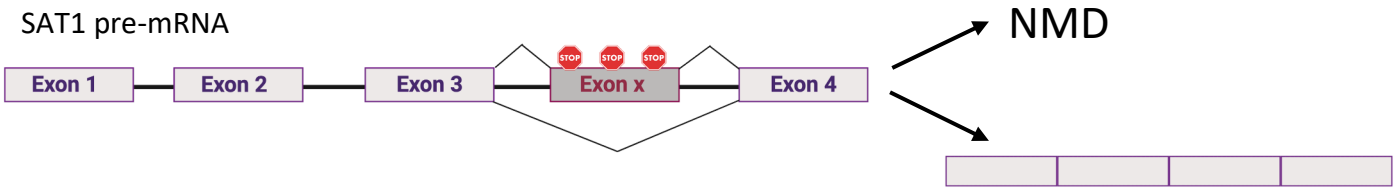
SAT1 pre-mRNA
Exon 1
Exon 2
Exon 3
Exon x
Exon 4
NMD

B.

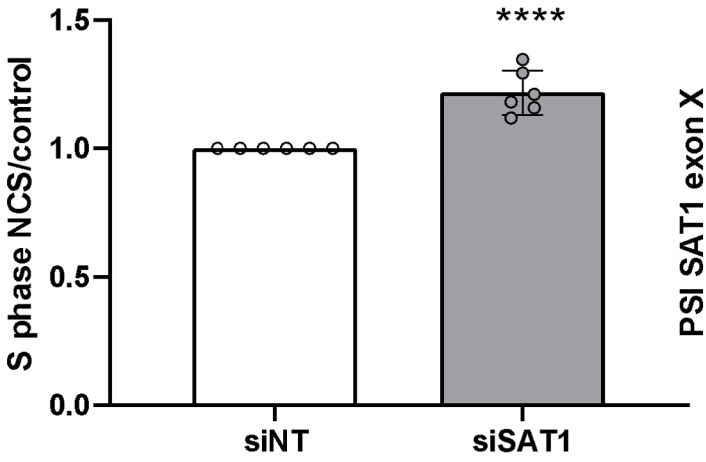
S phase NCS/control
1.5
1.0
0.5
0.0
****
siNT
siSAT1

C.

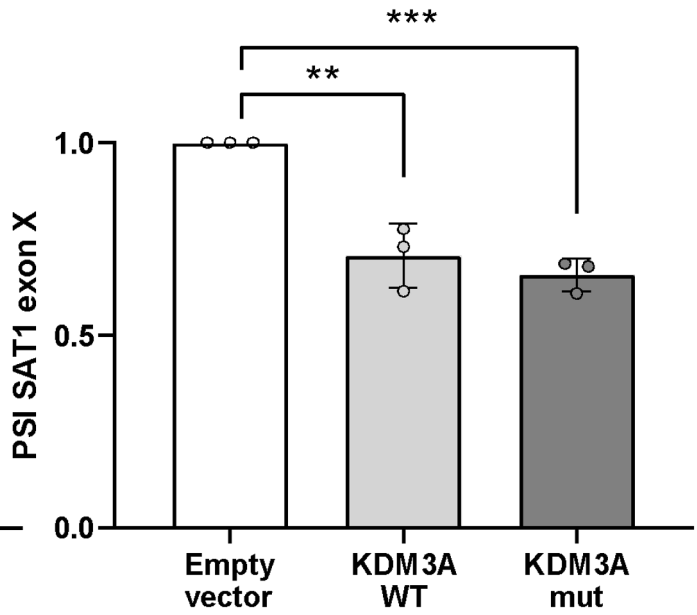
***
**
PSI SAT1 exon X
1.0
0.5
0.0
Empty vector
KDM3A WT
KDM3A mut

D.

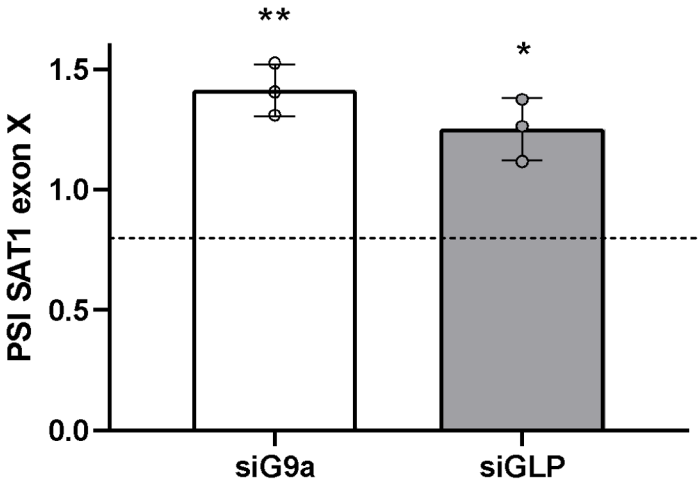
**
*
PSI SAT1 exon X
1.5
1.0
0.5
0.0
siG9a
siGLP

Fig 4.

A

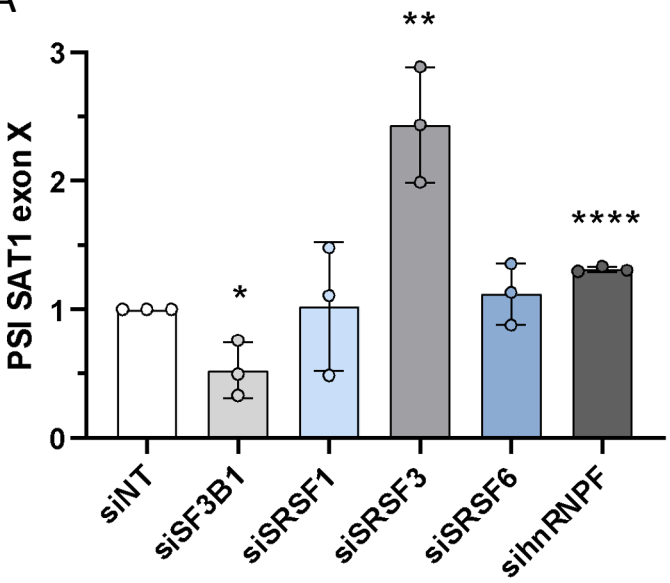
PSI SAT1 exon X
3
2
1
0
*
**
****
siNT
siSF3B1
siSRSF1
siSRSF3
siSRSF6
sihnRNPF

B

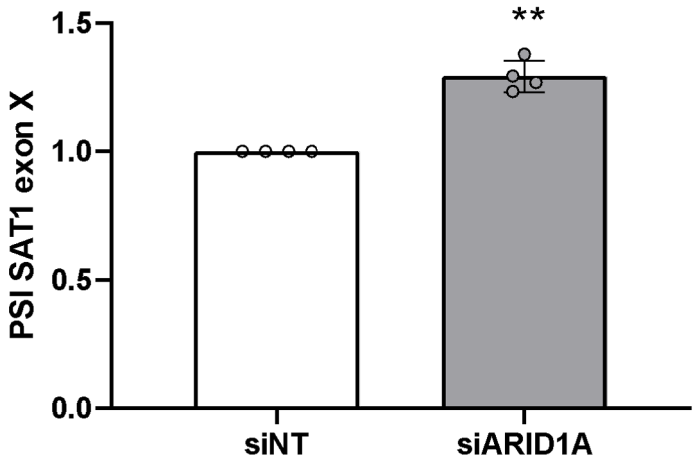
PSI SAT1 exon X
1.5
1.0
0.5
0.0
**
siNT
siARID1A

C

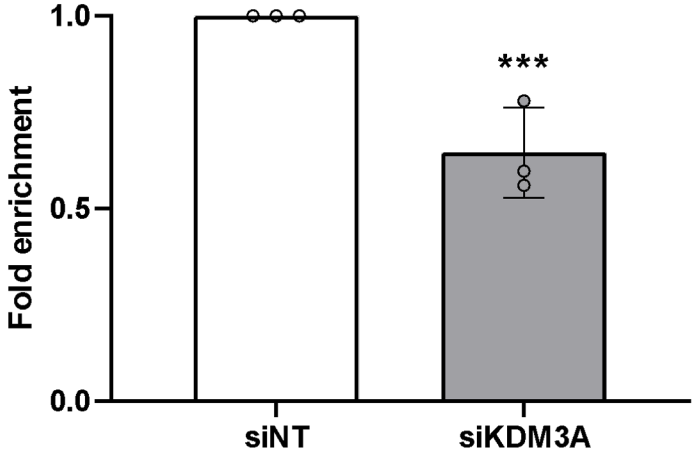
Fold enrichment
1.0
0.5
0.0
***
siNT
siKDM3A

Supplementary Fig. S1

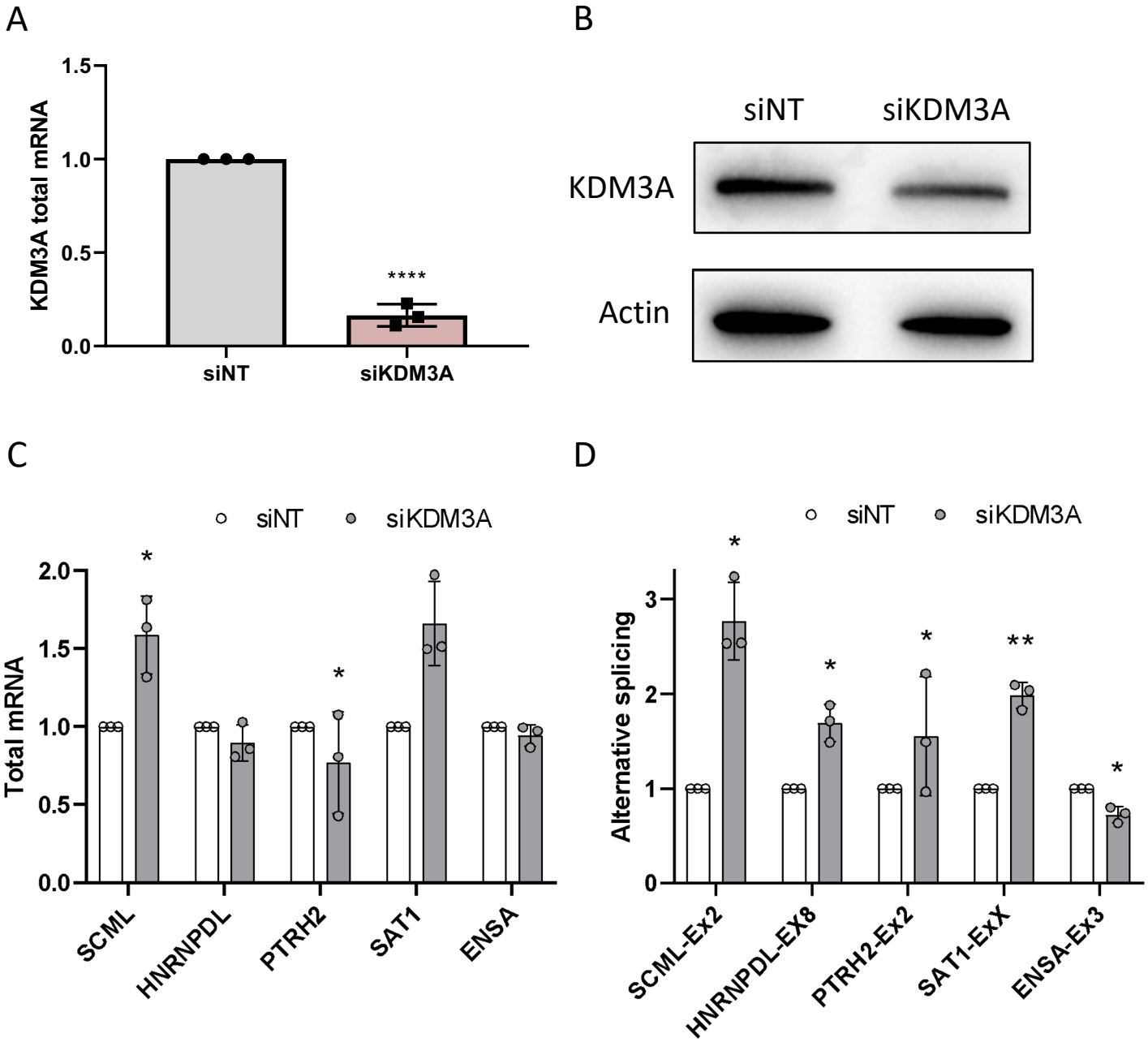

<u>Supplementary Figure S1.</u> A-D: MCF7 cells were transfected with non-targeting siRNA (siNT) and siKDM3A for 72 h. Total RNA was extracted and analyzed by real-time PCR for total mRNA amount of KDM3A (**A**). Immunoblotting was conducting using the indicated antibodies (**B**). Five genes (HNRNPDL, SAT1, SCML, PTRH2 and ENSA) were chosen for validation and total RNA was extracted and analyzed by real-time PCR for their total mRNA amount relative to *CycloA* reference gene (**C**); PSI of indicated genes was analyzed by real-time PCR relative to the total amount of that gene (**D**). Values represent averages of three independent experiments ±SD (* $p<0.05$; ** $p<0.01$; **** $p<0.0001$; Student's t test comparing to siNT).

Supplementary Fig. S2

A

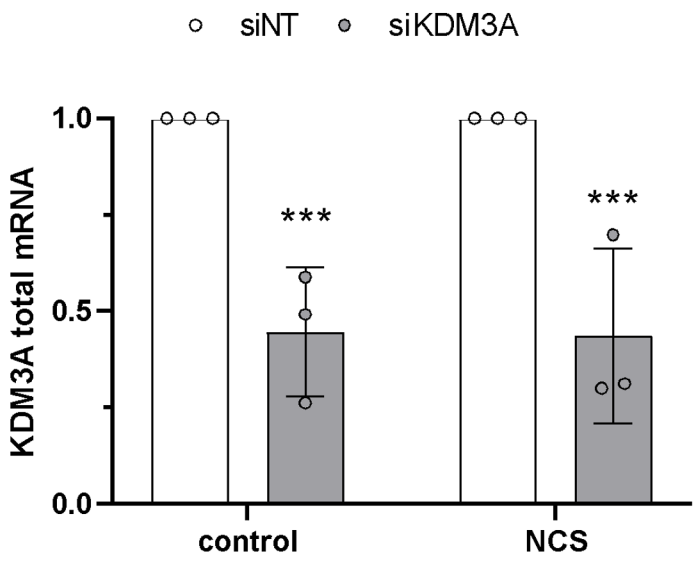

B

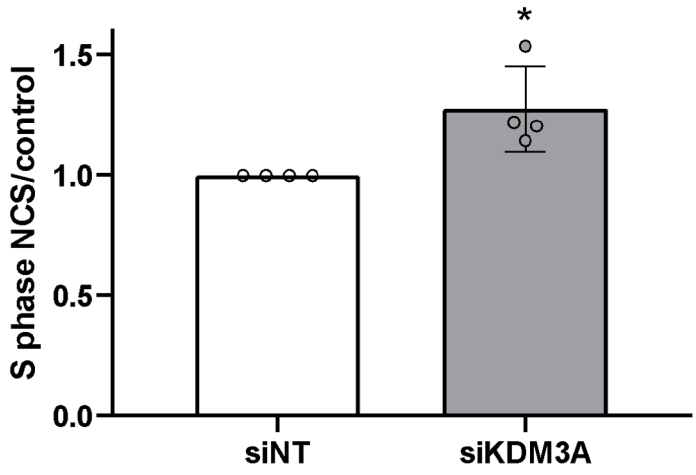

C

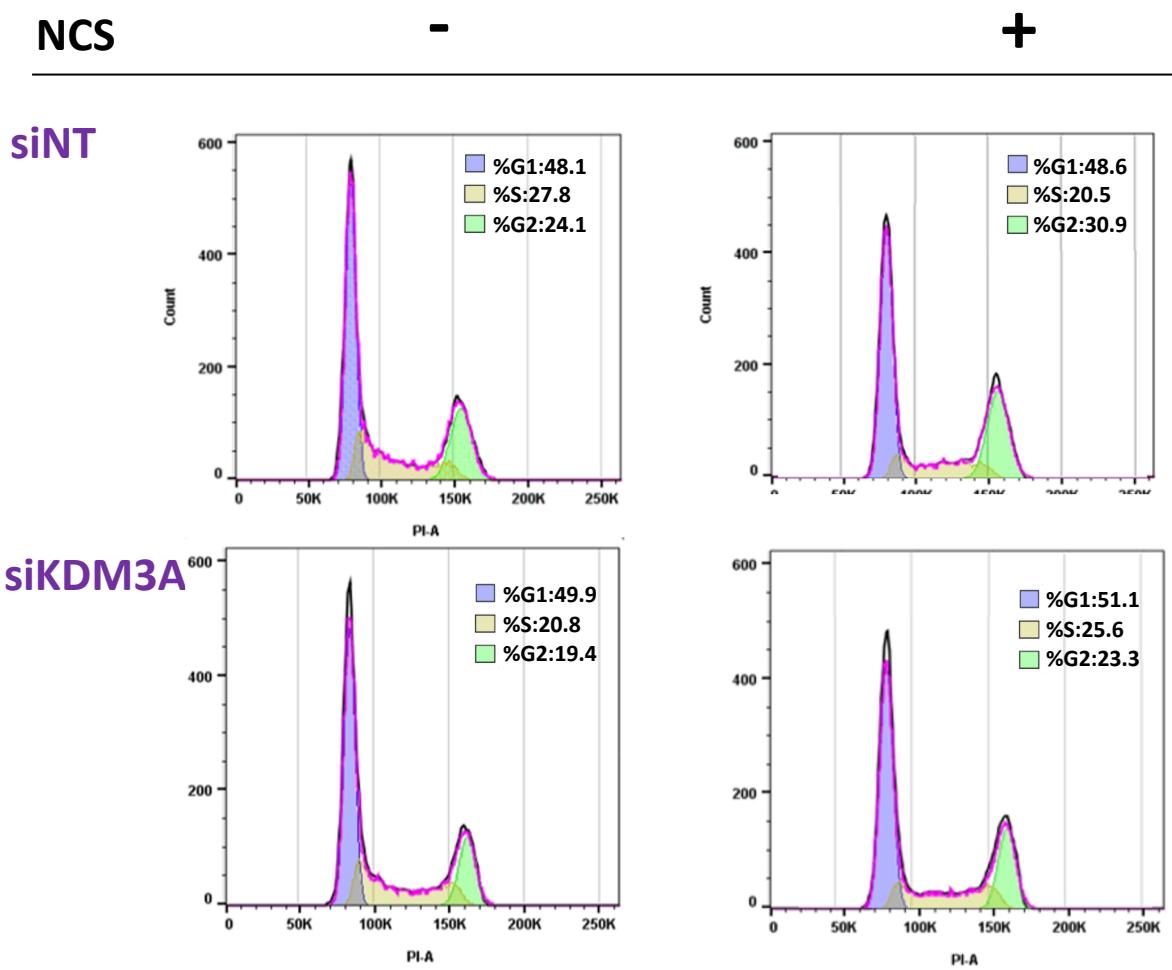

Supplementary Fig. S2, continued

D

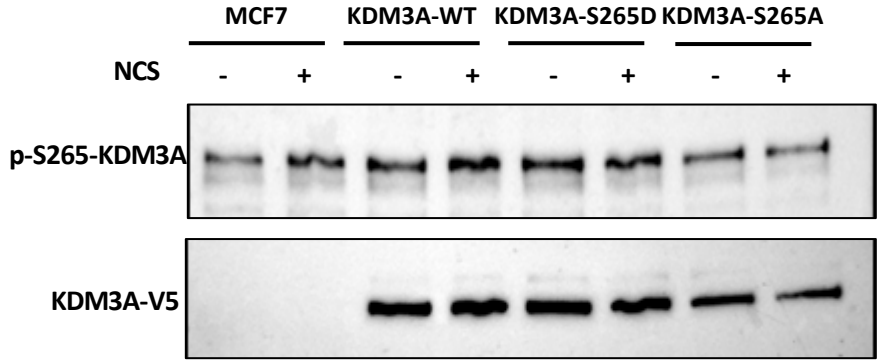

E

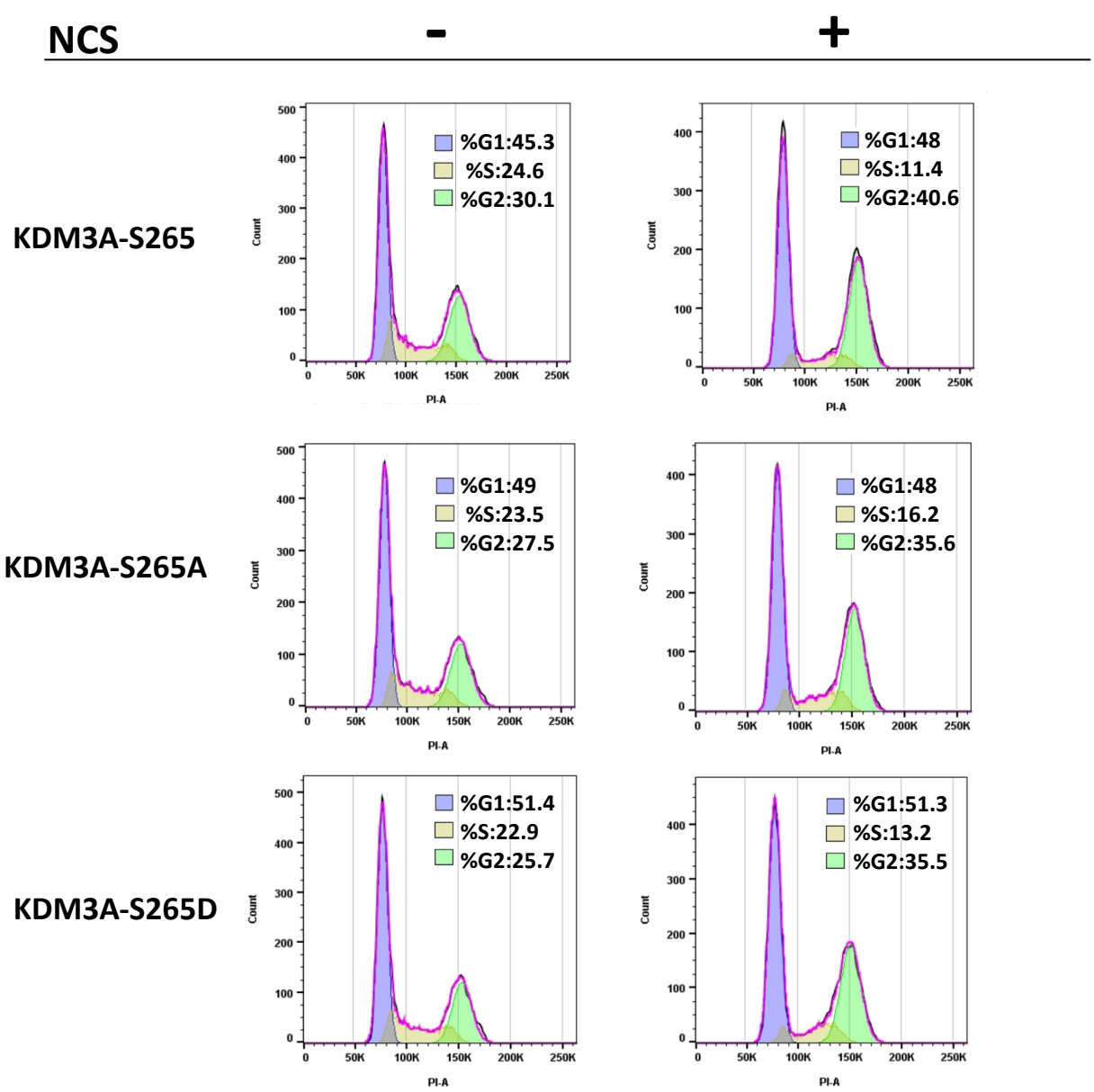

Supplementary Fig. S2, continued

F

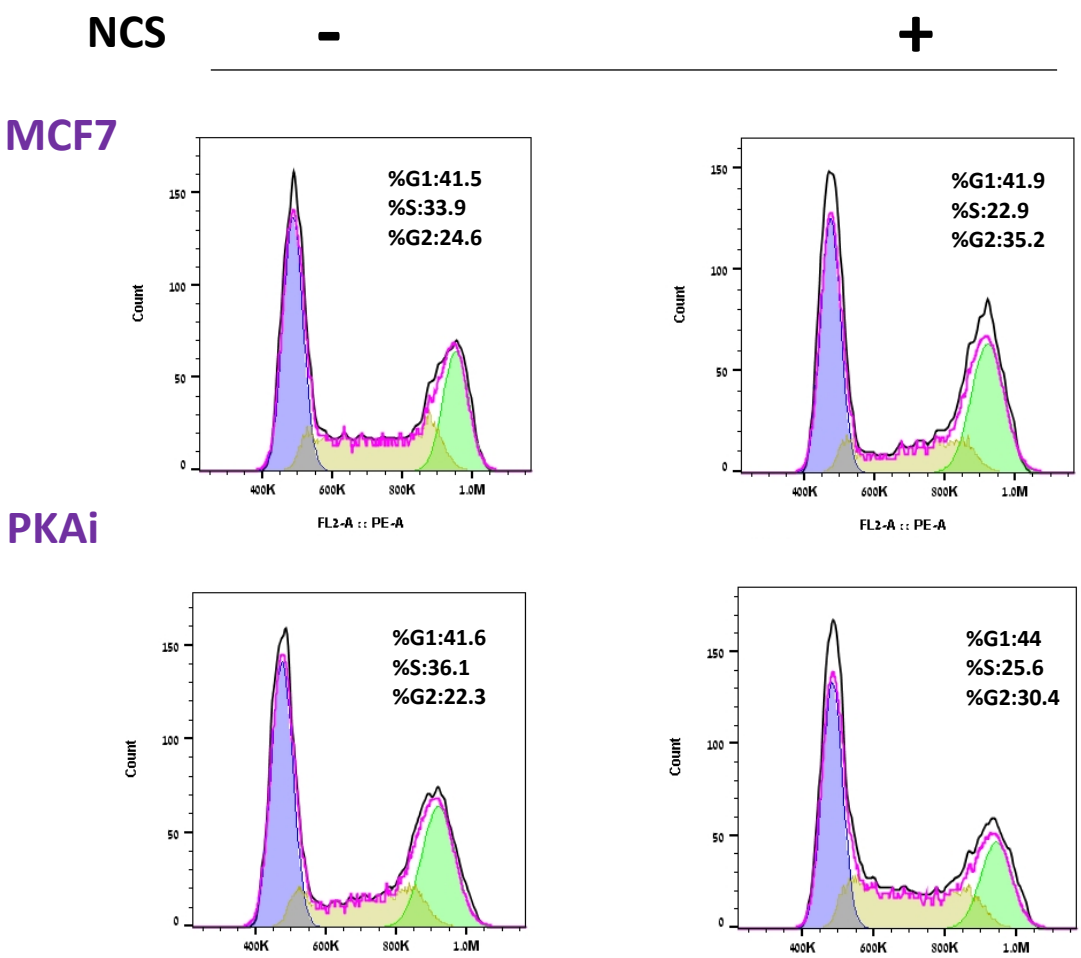

Supplementary Figure S2. **A-D**: MCF7 cells were transfected with non-targeting siRNA (siNT) and siKDM3A for 72 h and treated with 200 ng/ml NCS for 8 h. Total RNA was extracted and analyzed by real-time PCR for total mRNA amount of KDM3A relative to *CycloA* reference gene (**A**). Cells were analyzed using flow cytometry. The amount of cells accumulated in S-phase is shown as a fold-change relative to untreated cells (**B**). Values in **A** & **B** represent averages of three independent experiments ±SD (* $p<0.05$; *** $p<0.005$; Student's t test comparing to siNT). A population histogram for one representative experiment is shown (**C**). **D&E**. Protein was collected from MCF7 cells stably expressing either wild-type KDM3A or KDM3A mutated at serine 265 to alanine (S265A) or to aspartic acid (S265D). Immunoblotting was conducted with the indicated antibodies (**E**) and cells were treated with 200 ng/ml NCS for 8 h and analyzed using flow cytometry. A population histogram for one representative experiment is shown (**F**).

Supplementary Fig. S3

A

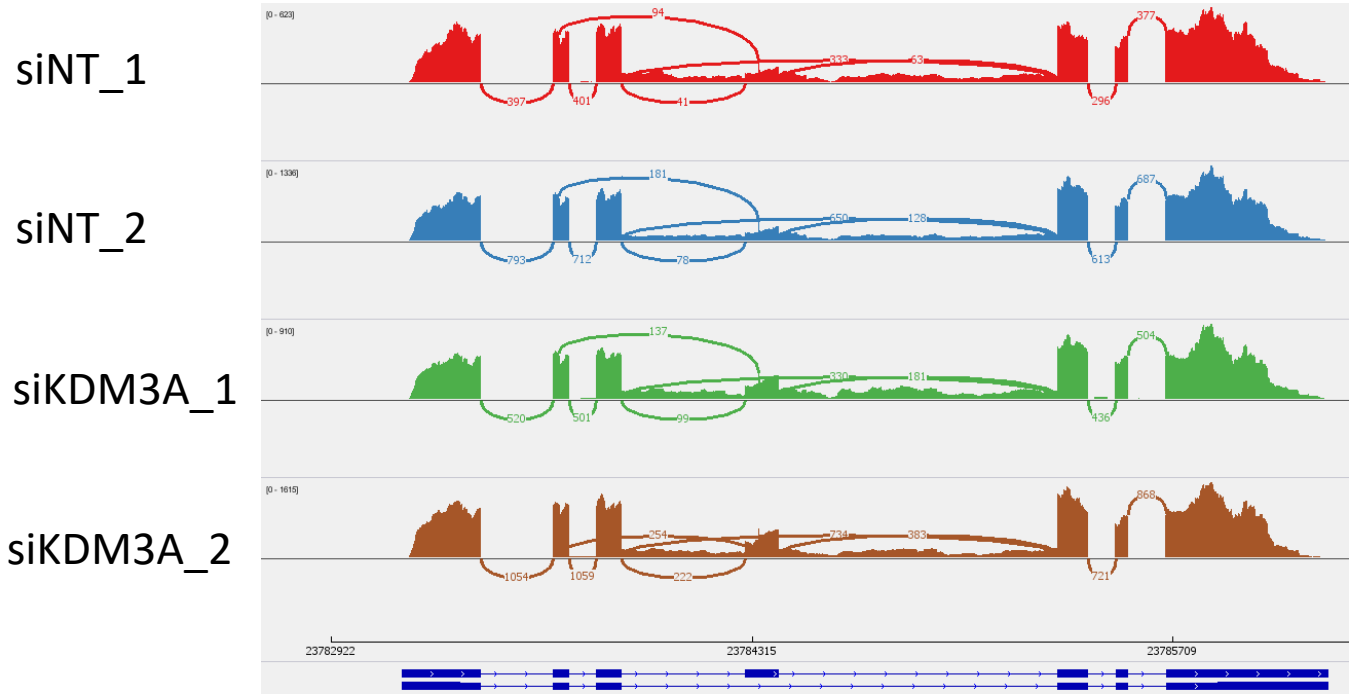

B

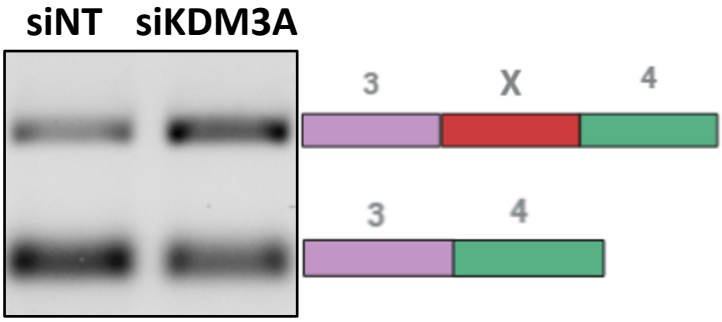

C

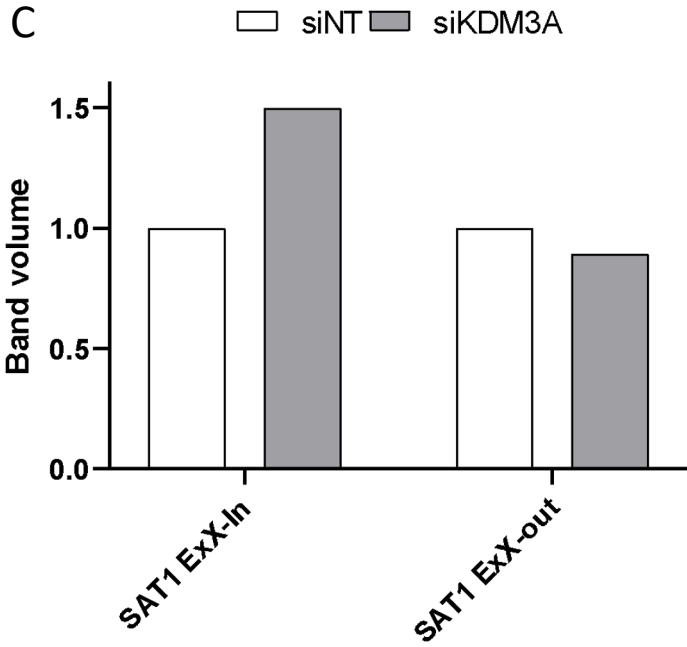

D

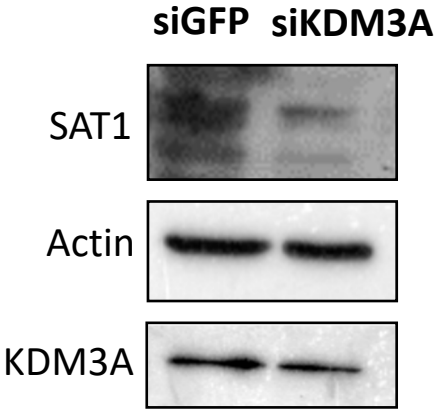

Supplementary Fig. S3

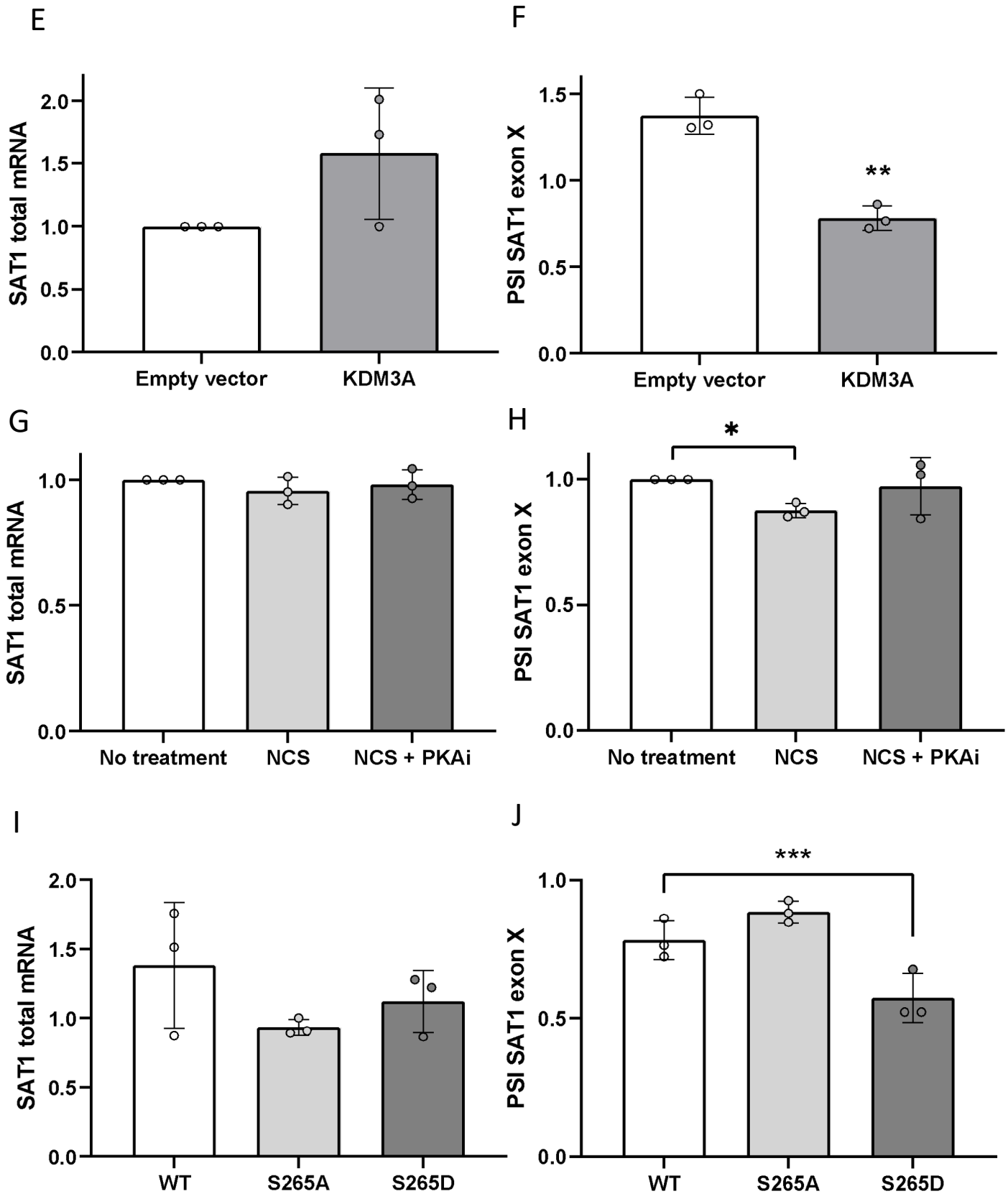

Supplementary Fig. S3, continued

K

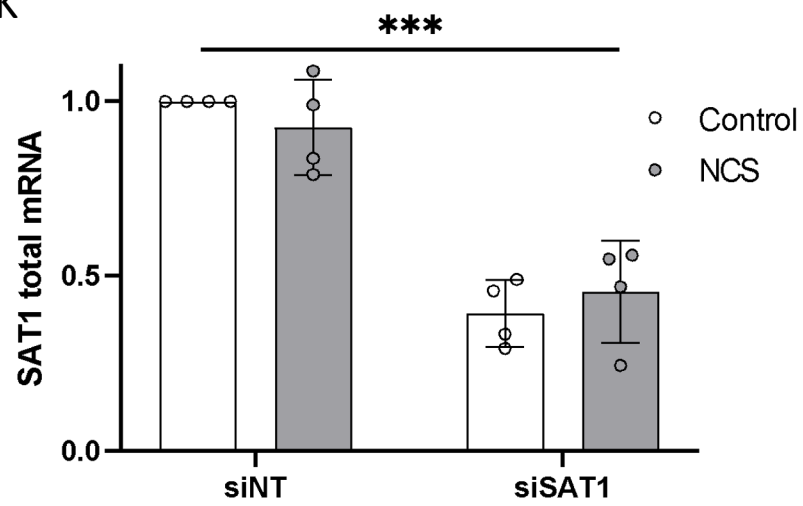

L

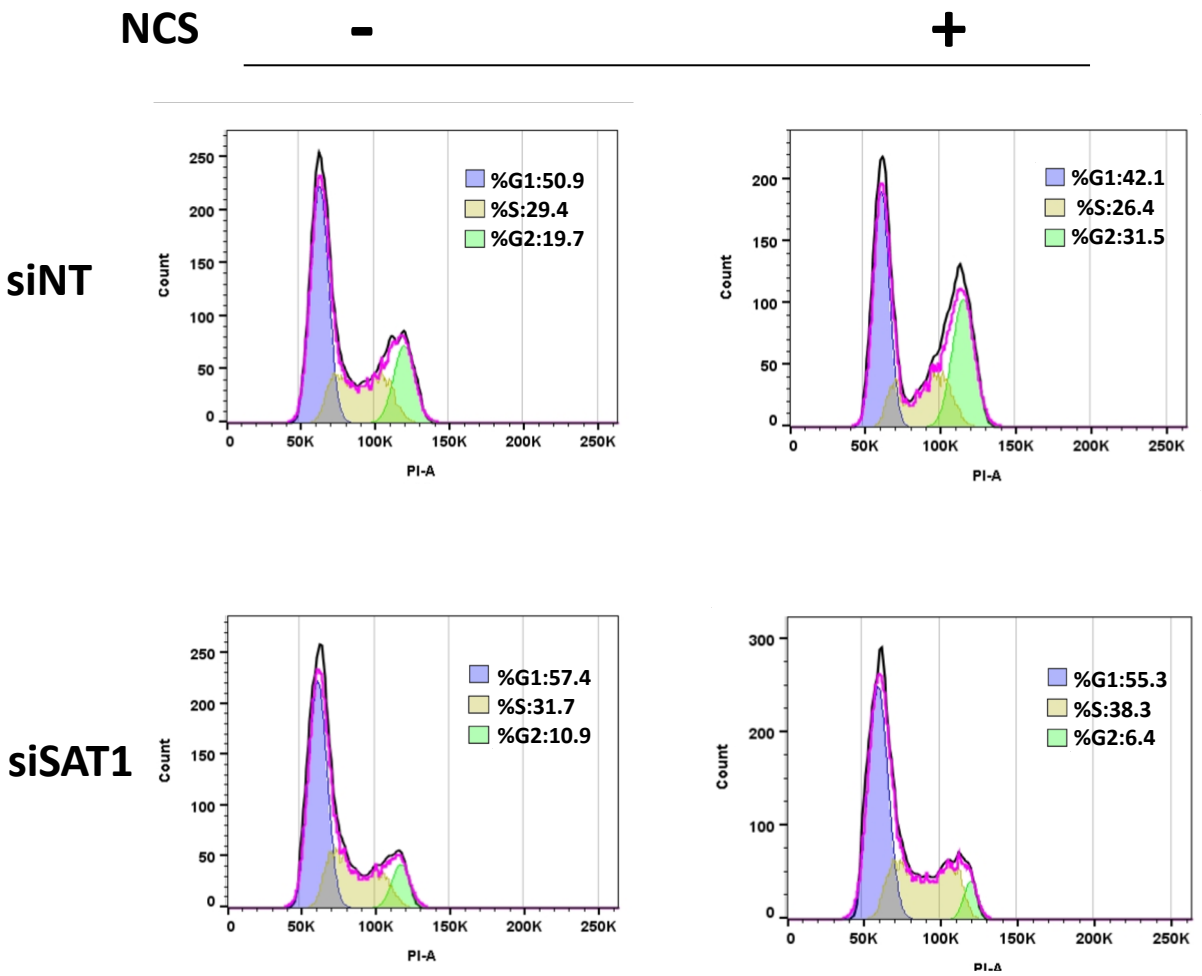

Supplementary Fig. S3, continued

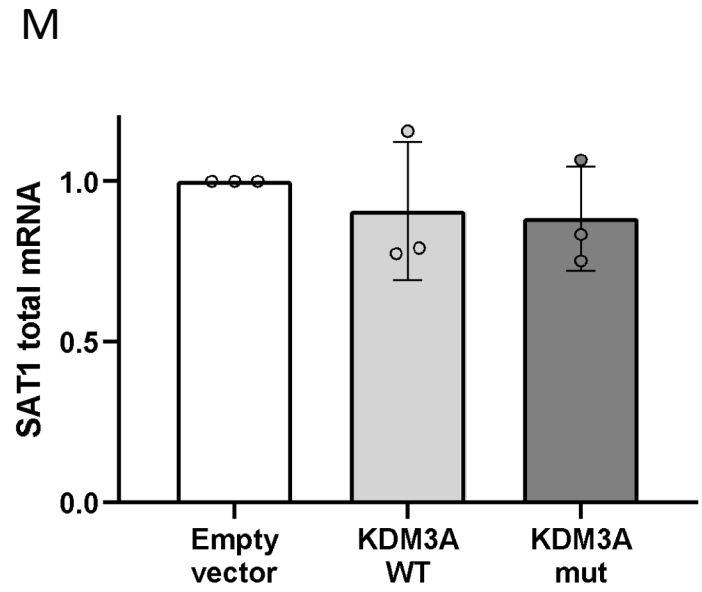

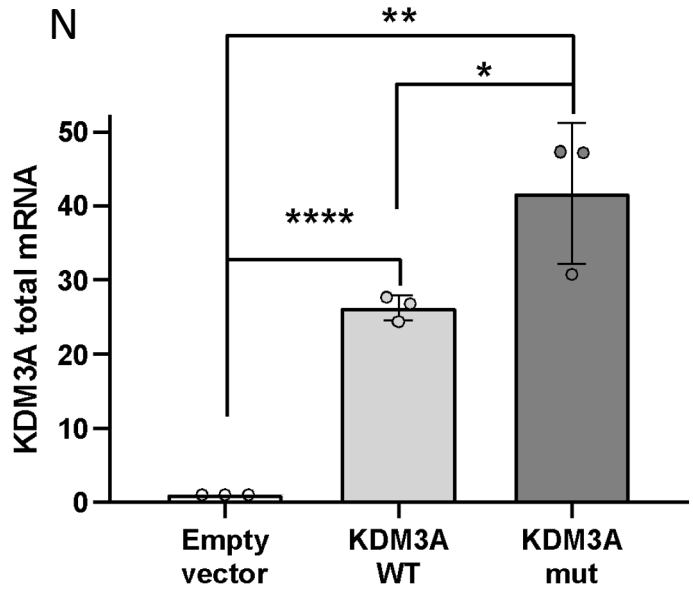

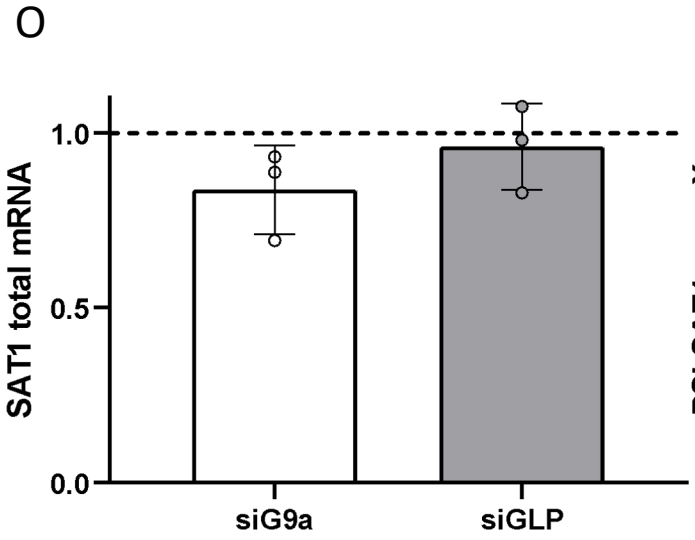

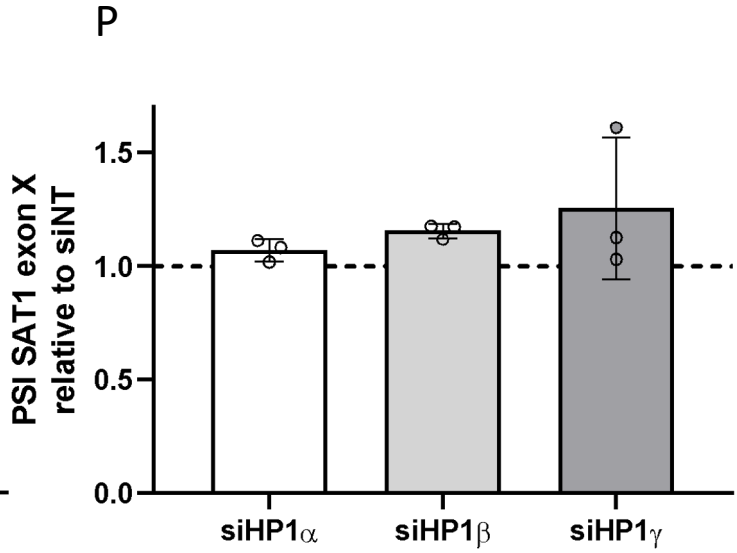

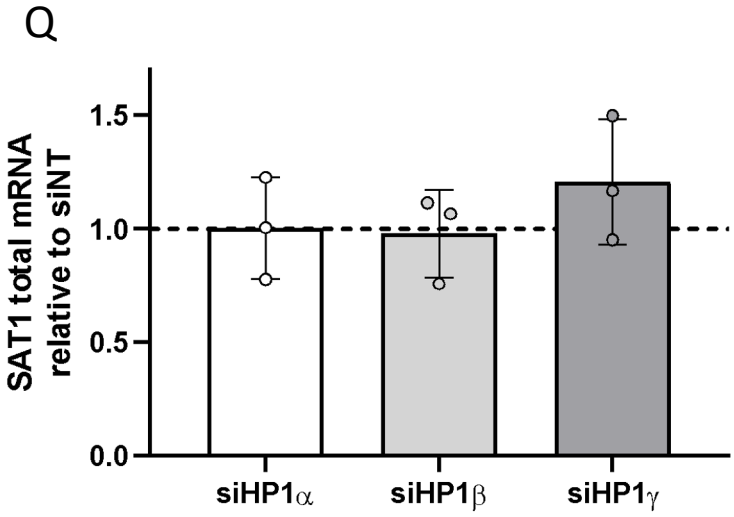

<u>Supplementary Figure S3</u>: **A**. RPKM for each alignment track are shown as sashimi plots (Katz *et al.* 2015). Arcs denote splice junctions, quantified in spanning reads, as specified near each exon junction of *SAT1* gene. **B & C**. SAT1 alternative splicing in MCF7 cells stably expressing either the empty vector or wild-type KDM3A. Total RNA was extracted and analyzed by real-time PCR for KDM3A relative to *CycloA* reference gene (**B**) and for SAT1 exon X inclusion. PSI was calculated by SAT1 exon X relative to SAT1 total mRNA amount (**C**). **D & E**. MCF7 cells were treated with PKAi for 30 minutes following by treatment with 200 ng/ml NCS for 1 h. Total RNA was extracted and analyzed by real-time PCR for SAT1 relative to *CycloA* reference gene (**D**) and for SAT1 exon X inclusion. PSI was calculated by SAT1 exon X relative to SAT1 total mRNA amount (**E**). **F & G**. SAT1 alternative splicing in MCF7 cells stably expressing either wild-type KDM3A or KDM3A mutated at serine 265 to alanine (S265A) or to aspartic acid (S265D). Total RNA was extracted and analyzed by real-time PCR for SAT1 relative to *CycloA* reference gene (**F**) and for SAT1 exon X inclusion. PSI was calculated by SAT1 exon X relative to SAT1 total mRNA amount (**G**). **H & I**. MCF7 cells were transfected with non-targeting siRNA (siNT) and siSAT1 for 72 h, total RNA was extracted and analyzed by real-time PCR for SAT1 relative to *CycloA* reference gene (**H**). Population histogram for one experiment is presented (**I**). **J & K**. SAT1 and KDM3A expression in MCF7 cells stably expressing either the empty vector, wild-type KDM3A or KDM3A mutated demethylase (mut). Total RNA was extracted and analyzed by real-time PCR for SAT1 relative to *CycloA* reference gene (**J**) and real-time PCR for KDM3A relative to *CycloA* reference gene (**K**). **L**. MCF7 cells were transfected with non-targeting siRNA (siNT) or siG9a, siGLP for 72 h. Total RNA was extracted and analyzed by real-time PCR for SAT1 relative to *CycloA* reference gene. **M & N**. MCF7 cells were transfected with non-targeting siRNA (siNT) or siHP1α, β, γ for 72 h, total RNA was extracted and analyzed by real-time PCR for SAT1 relative to *CycloA* reference gene (**M**) and for SAT1 exon X inclusion. PSI was calculated by SAT1 exon X relative to SAT1 total mRNA amount (**N**).

Supplementary Fig. S4

A

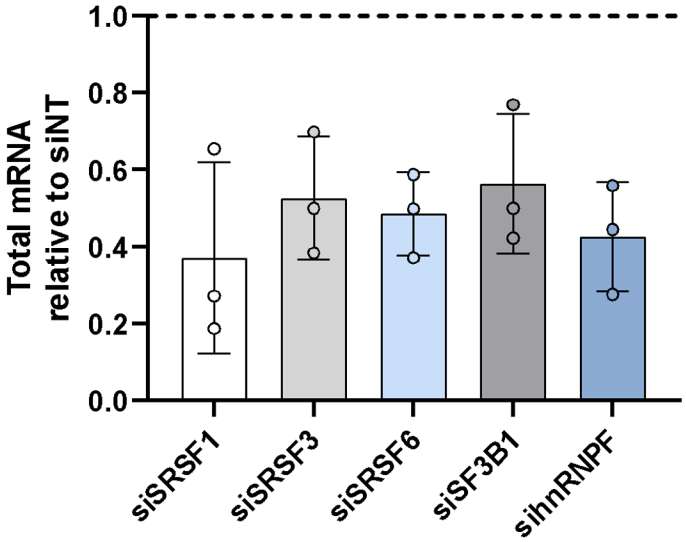

B

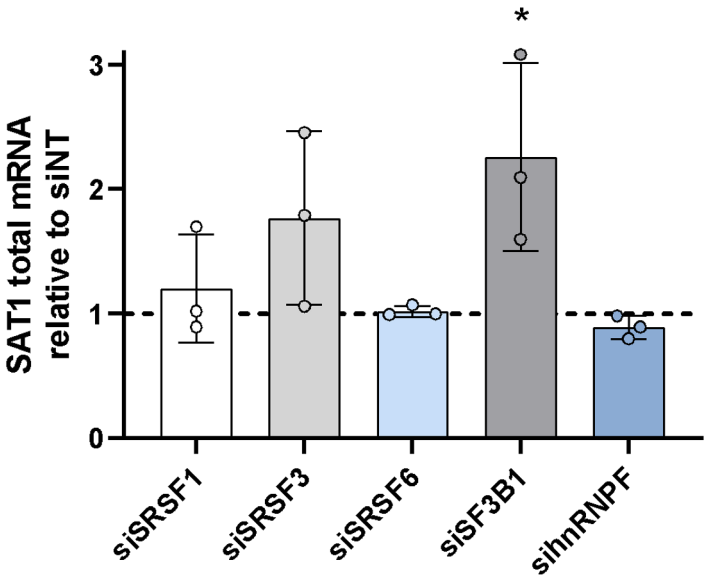

C

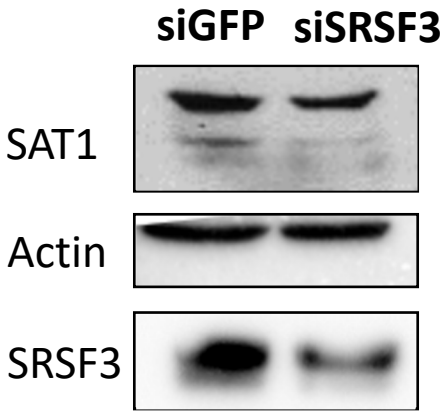

D

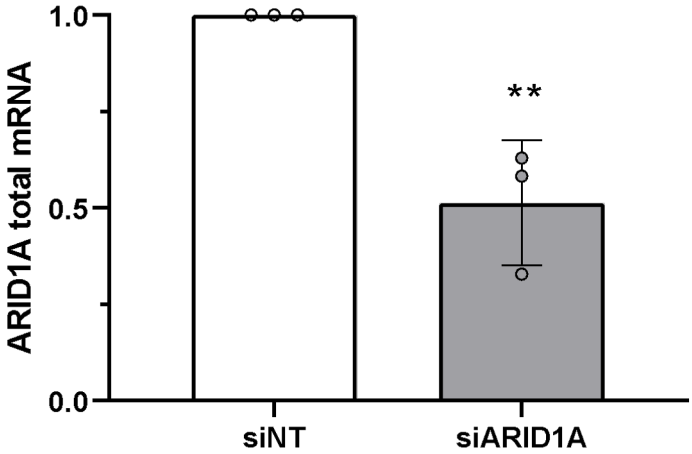

E

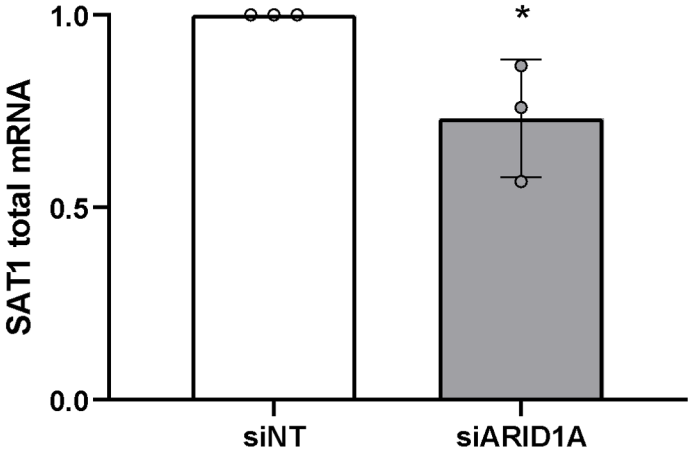

F

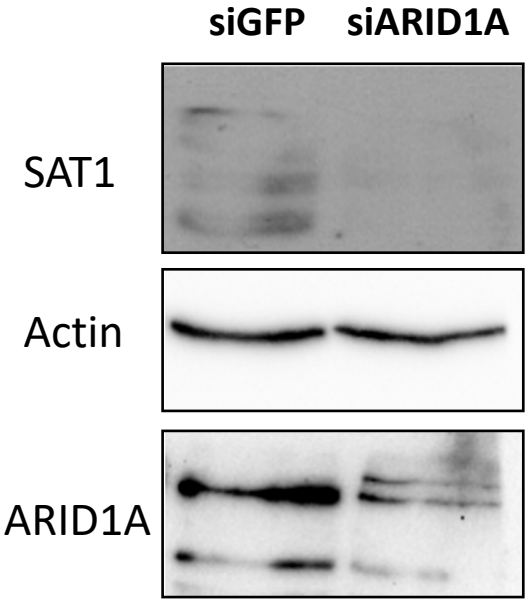

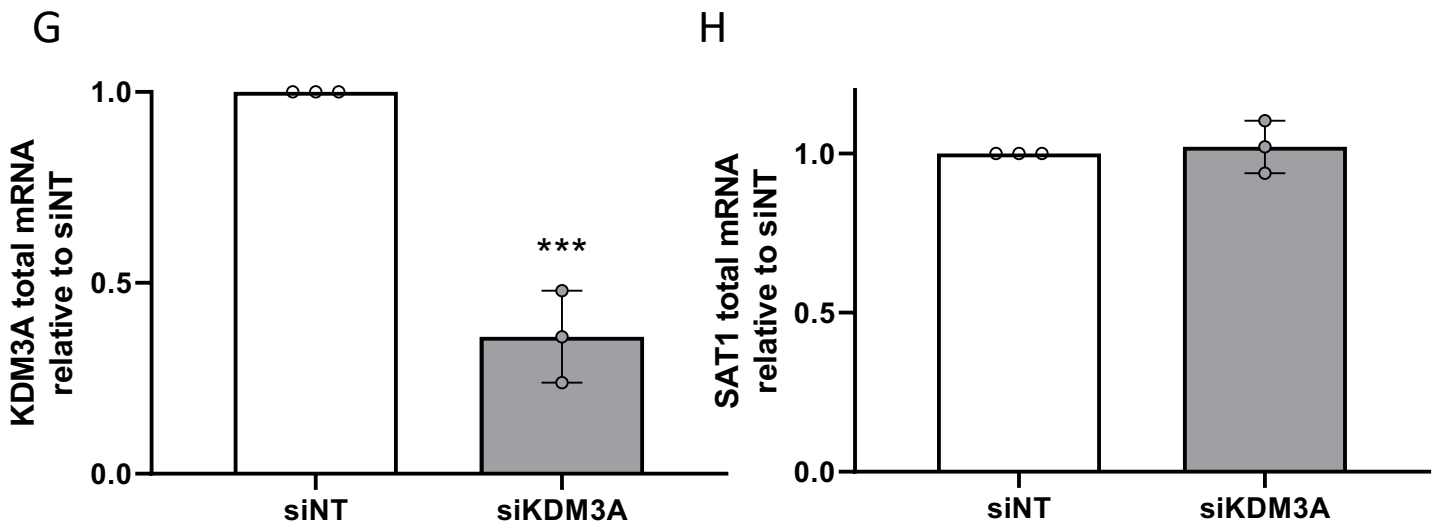

Supplementary Figure S4: **A-C**. MCF7 cells were transfected with non-targeting siRNA (siNT) or siSF3B1, siSRSF1/3/6 and sihnRNPF for 72 h. Total RNA was extracted and analyzed by real-time PCR for each gene relative to *CycloA* reference gene (**A**) and SAT1 relative to *CycloA* reference gene (**B**). Values in **A** & **B** represent averages of three independent experiments ±SD (* $p<0.05$; Student's t test comparing to siNT). Immunoblotting was conducting using the indicated antibodies (**C**). **D-F**. MCF7 cells were transfected with non-targeting siRNA (siNT) or siARID1A for 72 h. Total RNA was extracted and analyzed by real-time PCR for ARID1A (**D**) and for SAT1 (**E**) relative to *CycloA* reference gene. Values in **D** & **E** represent averages of three independent experiments ±SD (* $p<0.05$, ** $p<0.01$; Student's t test comparing to siNT). Immunoblotting was conducting using the indicated antibodies (**F**). **G&H**. MCF7 cells were transfected with non-targeting siRNA (siNT) or siKDM3A for 72 h. Total RNA was extracted and analyzed by real-time PCR for KDM3A (**G**) and for SAT1 (**H**) relative to *CycloA* reference gene. Values in **G** & **H** represent averages of three independent experiments ±SD (*** $p<0.001$; Student's t test comparing to siNT).

Supplementary table S1. Primer used in this study		
Primer name	**Description**	**Sequence**
F-CycloA	Endogenous control for qPCR	GTCAACCCCACCGTGTTCTT
R-CycloA		CTGCTGTCTTTGGGACCTTGT
F-KDM3A	Total KDM3A mRNA	TGAGCCACACAGACAGGTTG
R-KDM3A		CAGCACCCTGTTGGCAATTC
F-G9a	Total G9a mRNA	CTGTCAGAGGAGTTAGGTTCTGC
R-G9a		CTTGCTGTCGGAGTCCACG
F-SAT1	Total SAT1 mRNA	TGTTTATCCGTCACTCGCCG
R-SAT1		TTTAGCCAGCTCCTTGATCAGC
F-SAT1-ExX	SAT1 isoform	TCCGTGTACATGGATGGGC
R-SAT1-Ex4		ATGGCAAAACCAACAATGCT
F-SRSF1	Total SRSF1 mRNA	AGTGGTTGTCTCTGGACTGC
R-SRSF1		ACCACTGTATCCAATTCTGGTCAA
F-SRSF3	Total SRSF3 mRNA	CTGATGCAGTCCGAGAGCT
R-SRSF3		ACCATTCGACAGTTCCACTC
F-SRSF6	Total SRSF6 mRNA	CCACGCACAAGCCATAGGCGAT
R-SRSF6		CGACCTGGAACGGGAGCGACT
F-SF3B1	Total SF3B1 mRNA	TGCAGATGGCTTCTATTCTGCTGC
R-SF3B1		GGGTTCCTGGGTTGCTAATCCGG
F-hnRNPF	Total hnRNPF mRNA	CGCCTCCGTGGACATTTCAT
R-hnRNPF		GGAAGTTCTGCACGTCCTCA
F-HP1-gamma	Total HP1-gamma mRNA	AGTGGTCCCAAAGGGGTACT
R-HP1-gamma		AGAGCTATTACGTTCGCGGC
F-HP1-alpha	Total HP1-alpha mRNA	TCCTGTTAGCCCAGAGGGAA
R- HP1-alpha		TGTGCTCCTCAGAAAAGCCT
F-HP1-Beta	Total HP1-Beta mRNA	GCA AACCAAAGAAGAAGAAAGA
R-HP1-Beta		ATAATCCGCTCCGGCTCCAAA
F-ARID1A	Total ARID1A mRNA	GAGATTGGTGGATTGACTCAG
R-ARID1A		GTTGCAAGTTCCCGCCATT
F-ENSA-Ex3	ENSA isoform	GCTTCTCTGTGCGGATGAAATG
R-ENSA-Ex4		GTGATCACCAGTCACCAGGTTC
F-ENSA	Total ENSA mRNA	TACAACATGGCCAAAGCCAAG
R-ENSA		TGGTGACGAGCGAGGACTT
F-SCML-Ex1	SCML isoform	CGTGACAGGCTCTGTCACTAA
R-SCML-Ex2		CACATCGATTTCACTGGAGCTG
F-SCML	Total SCML mRNA	AACTGACCATGCTTCTGCAGCA
R-SCML		AAGGGTGCTTAGTGATGCTTCC
F-HNRNPDL-Ex7	HNRNPDL isoform	CCAGCCATACTAAAGGAGAAC
R-HNRNPDL-Ex8		CACAGGACAGCGTTTTCTGGT
F-HNRNPDL	Total HNRNPDL mRNA	CGAGCAAGAATCAGCAGGATGA
R-HNRNPDL		GCTTGTATCCCAGCTCAAGCC
F-PTRH2-Ex1	PTRH2 isoform	GTGAGGAAAGGAGGTACTGTAG
R-PTRH2-Ex2		CTGAATGGGTGTCTCTTTCACAC
F-PTRH2	Total PTRH2 mRNA	TTGGAGTTGCTTGTGGCATGTG
R-PTRH2		GCTGTCTCCCAAGATGCTTGC
F-SAT1-intron 3	RIP primer to check SAT-ExX	TTGACCCTAACGTAACAGTTTT
R-SAT1-ExX		AGGATCTTTTAGTTACCTCCCC